PFC/RR-82-34

DOE/ET-51013-62
UC20

NUMERICAL MODELING OF A FAST NEUTRON COLLIMATOR FOR THE "ALCATOR A" FUSION DEVICE

William Andrew Fisher

Plasma Fusion Center
Massachusetts Institute of Technology
Cambridge, MA 02139

December 1982

This work was supported by the U.S. Department of Energy Contract No. DE-AC02-78ET51013. Reproduction, translation, publication, use and disposal, in whole or in part by or for the United States government is permitted.

NUMERICAL MODELING OF A FAST NEUTRON COLLIMATOR FOR THE "ALCATOR A" FUSION DEVICE

by

WILLIAM ANDREW FISHER

B.S.E.P., The Ohio State University
(1977)

SUBMITTED IN PARTIAL FULFILLMENT

OF THE REQUIREMENTS FOR THE

DEGREE OF

MASTER OF SCIENCE

at the

 MASSACHUSETTS INSTITUTE OF TECHNOLOGY

January 1980

Signature of Author William A Fisher
Department of Nuclear Engineering, January 18, 1980

Certified by Lawrence M Lidsky
Lawrence M. Lidsky, Thesis Supervisor

Certified by Kent F. Hansen
Kent F. Hansen, Thesis Co-Supervisor

Accepted by _____
Chairman, Department Committee

NUMERICAL MODELING OF A FAST NEUTRON COLLIMATOR FOR THE "ALCATOR A" FUSION DEVICE

by

WILLIAM ANDREW FISHER

Submitted to the Department of Nuclear Engineering on January 18, 1980 in partial fulfillment of the requirements for the Degree of Master of Science

ABSTRACT

A numerical procedure is developed to analyze neutron collimators used for spatial neutron measurements of plasma neutrons. The procedure is based upon Monte-Carlo methods and uses a standard Monte-Carlo code. The specific developments described herein involve a new approach to represent complex spatial details in a method that is conservative of computer time, retains accuracy and requires only modest changes in already developed Monte-Carlo procedures.

The procedure was used to model the Alcator A collimator. The collimator consists of 448 cells and has a measured spatial point source response of 0.7cm. The numerical procedure successfully predicts this response.

Thesis Advisor:	Lawrence M. Lidsky
Title:	Professor of Nuclear Engineering
Co-Advisor:	Kent F. Hansen
Title:	Associate Dean of Engineering

TABLE OF CONTENTS

Table of Contents (continued)

LIST OF FIGURES

LIST OF TABLES

ACKNOWLEDGEMENT

This work was done during a period of 10 months beginning in March 1979, supported initially by the Department of Nuclear Engineering's fund for unsponsored research and later by the Confinement Studies group of the Alcator Fusion Group at the Francis Bitter National Magnet Laboratory. I would like to thank my co-advisors, Professor L.M. Lidsky and Dean K. Hansen for their help, encouragment and review, particularly in the final stages of this thesis. I would also like to thank Dale Lancaster for his help in cross-section selection, Rachel Morton for her help in obtaining the ANDY code, and Cathy Lydon for her expedient typing of this work. In particular, I would like to thank Dave Gwinn who suggested this topic, for his discussions and assistance.

CHAPTER 1. INTRODUCTION

1.1 Thesis Statement and Objectives

The purpose of this thesis is to model mathematically the fast neutron collimator used to measure spatial neutron profiles on the Alcator A fusion device. The measurement of these profiles provides information on some of the mechanisms of plasma heating.

The mathematical model provides the means to analyze critical collimator parameters, which are difficult or impossible to measure directly. For example, it is difficult to obtain energy information on the neutrons emerging from the collimator by measurement, while such information is easily obtained in Monte-Carlo type models. In fact, a Monte-Carlo type model can provide the neutron energy distribution anywhere in the collimator. This information is not only useful in the analysis of the present collimator, but also in the design optimization of future collimators.

1.2 Properties of Fast Neutron Collimators

The purpose of a fast neutron collimator is to establish the position of a fast neutron source and in the case of a fusion plasma, to measure the spatial distribution of the neutron production in the plasma. In designing a collimator to accomplish this purpose the criteria of spatial resolution, detector solid angle, and neutron transport need to be examined carefully. Although the emphasis of this thesis is the modeling of neutron transport

characteristics it is useful to understand the criteria under which the Alcator "A" collimator was designed.

1.2.1 Spatial Resolution

The spatial resolution of a collimator is its ability to resolve differences in neutron production as a function of position. The figure of merit in the case of resolution is the full width at half maximum (fwhm) of the spectrum obtained when a point source is scanned. An order of magnitude estimate of the fwhm response can be obtained by considering the limiting rays of the collimator as in Figure 1.1. The resolution in that case is given by

$$\Delta X = (X_2 + X_1)d/l + X_1 \qquad 1.1$$

where the symbols are defined in Figure 1.1.

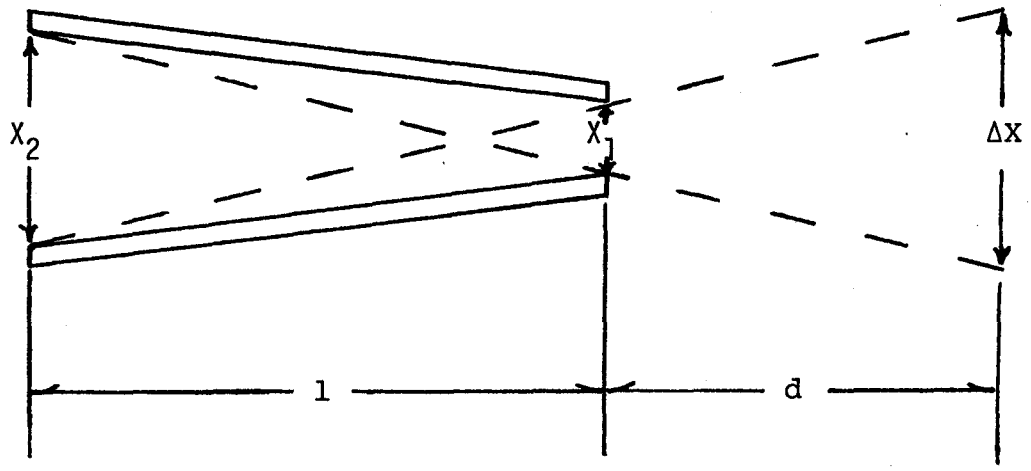

Figure 1.1 Limiting rays of a collimator

In general the spatial resolution should be two to three times smaller than the structure to be resolved.

In the case of an Alcator plasma the neutron production profile is strongly dependent on the ion temperature and density profiles. Using typical profiles for density and ion temperature the neutron production profile has the form[1]

$$n(r) = n_o \exp[-r^2/1.9] \qquad 1.2$$

where r is in cm. In order to resolve this structure one would need a spatial resolution of about 1 cm fwhm.

1.2.2 Solid Angle

Detector solid angle, the second criteria, is of great importance in order to maximize the detector count rate. The solid angle is normally given in terms of a geometric efficiency, ε_g, where

$$\varepsilon_g = Ad/4\pi r^2 \qquad 1.3$$

Ad is the area of the detector and r the distance from a point source. The value of r is fixed by neutron transport properties and in the case of the Alcator collimator is equal to about 2 meters. Unfortunately, in the case of a single cell collimator increasing Ad degrades the spatial resolution. This can be seen by again considering

Equation 1.1. Increasing Ad implies one increases X_2 and X_1 resulting in a larger ΔX. The multicell collimator used for the Alcator measurement and shown in Figure 1.2, circumvents this problem. The small component collimator cells maintain high resolution but view a small solid angle, while a large number of cells can be used to increase the solid angle.

1.2.3 Neutron Transport

A third area of concern in the design of a collimator is neutron transport in the construction material. An ideal collimator would absorb all neutrons outside good geometry. In that case the resolution of the collimator for a source a distance d from the collimator is given by the extent of the limiting rays, ΔX, in Equation 1.1. Unfortunately, there is no known material which acts as a perfect absorber. In fact in the case of fast neutrons (2.5 Mev) the capture cross-sections are very small and are generally more than an order of magnitude smaller than the corresponding elastic scattering cross-section.[2] This forces the requirement that any fast neutron collimator will have a large component of elastic scattering and thus must depend on slowing down and then capture rather than a straight-forward capture scheme. The problem is further complicated by the constraint that the neutron looses on an average less than one half of its original energy in one

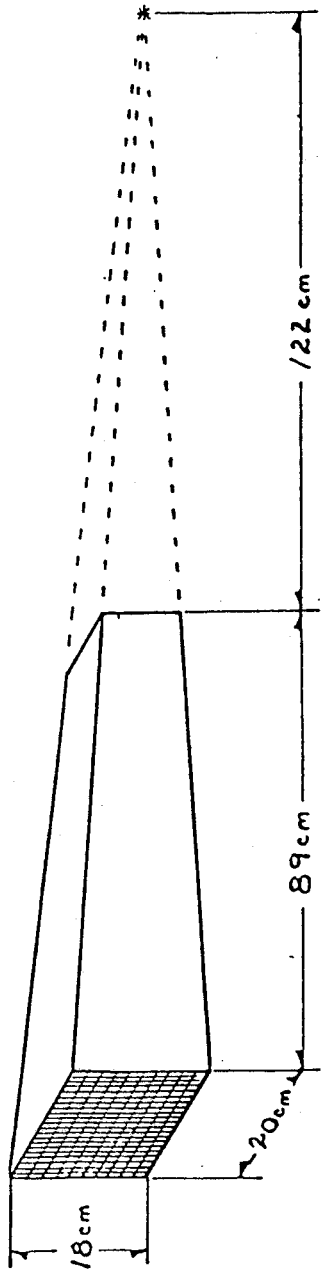

Figure 1.2 Alcator Multicell Collimator

collision (E_{ave} = 0.5 for hydrogen). Table 1.1 summarizes the ratio E_{out}/E_{in} for hydrogen as a function of the center of mass scattering angle, θ_c. The number of collisions at that angle required to reduce the incident neutron energy below $0.1(E_{in})$ has also been tabulated.

θ_c(degrees)	E_{in}/E_{out}	# of collision for $0.1E_n$
0	1.0	
5	0.998	1200
10	0.992	300
20	0.970	130
30	0.933	75
45	0.853	14
60	0.750	8
90	0.500	3
143	0.101	1

TABLE 1.1 E_{in}/E_{out} vs θ_c for Hydrogen

In the case of hydrogen $\theta_{lab} = 1/2\theta_c$ and scattering is essentially isotropic below 2.5 Mev.[2] Although the average energy of all the neutrons taken together is $(0.5)^3 E_{in} = 0.125\ E_{in}$ after three collisions, the neutrons in the forward direction, which have the highest probability of reaching the detector suffer a much lower energy loss. Therefore, more than three collisions would be required to reduce E_{ave} forward below $0.1\ E_{in}$. Because

the number of collisions is large and unknown one cannot, using Table 1.1, predict the average energy of neutrons at the exit of the collimator. In designing a collimator one needs to know the number and energy of neutrons which emerge from the collimator due to scatterings from bad geometry. The idea behind the Alcator collimator is to make the collimator long enough to assure that even neutrons which are scattered initially in the forward direction eventually experience a collision which reduces the energy enough to assure it can be discriminated against at the detector. Thus it appears that the longer the collimator is, the closer it approaches the ideal absorber case, in which only neutrons in good geometry would be detected. The Alcator collimator is very close to this criteria.

1.3 The Alcator Collimator

The Alcator collimator, shown previously in Figure 1.2 consists of 448 high resolution collimator cells arranged so that the center line of each cell goes through a focal point 122cm in front of the collimator. The inside dimensions of each component cell are 0.3903cm (Y), 0.9393cm (X), at the large end, the detector end, and 0.1588cm (Y), 0.4763cm (X) at the small end, the source end. The wall thickness is 0.159cm (1/16 of an inch). There are 32 cells

in the Y direction and 14 cells in the Y direction. These dimensions yield a limiting ray divergence at the focal point of 0.912cm in the Y direction and 2.42cm in the X direction.

The length of the collimator is 88.9cm. This provides about 10 mean free paths of scattering in the plexiglass construction material.

Figure 1.3 shows the collimator in the experimental set-up next to Alcator A. The front of the collimator is 122cm from the center of the plasma column (the focal length). A 2.13 meter (7.0 feet) diameter tank utilizing water as a neutron shield provides 6 orders of magnitude attenuation of background scattered neutrons. A Helium-3 proportional counter tube in a cadmium wrapped moderator is used as the fast neutron detector.

1.4 Numerical Modeling

As was pointed out in the discussion of neutron transport properties a large and unknown number of collisions are needed to provide good collimation. This makes a straight forward analytical derivation of the neutron energy and spatial distributions formidable and a Monte Carlo based modeling is best suited to this problem.

In the Monte-Carlo method the neutron is given an initial position and an initial velocity and then allowed to

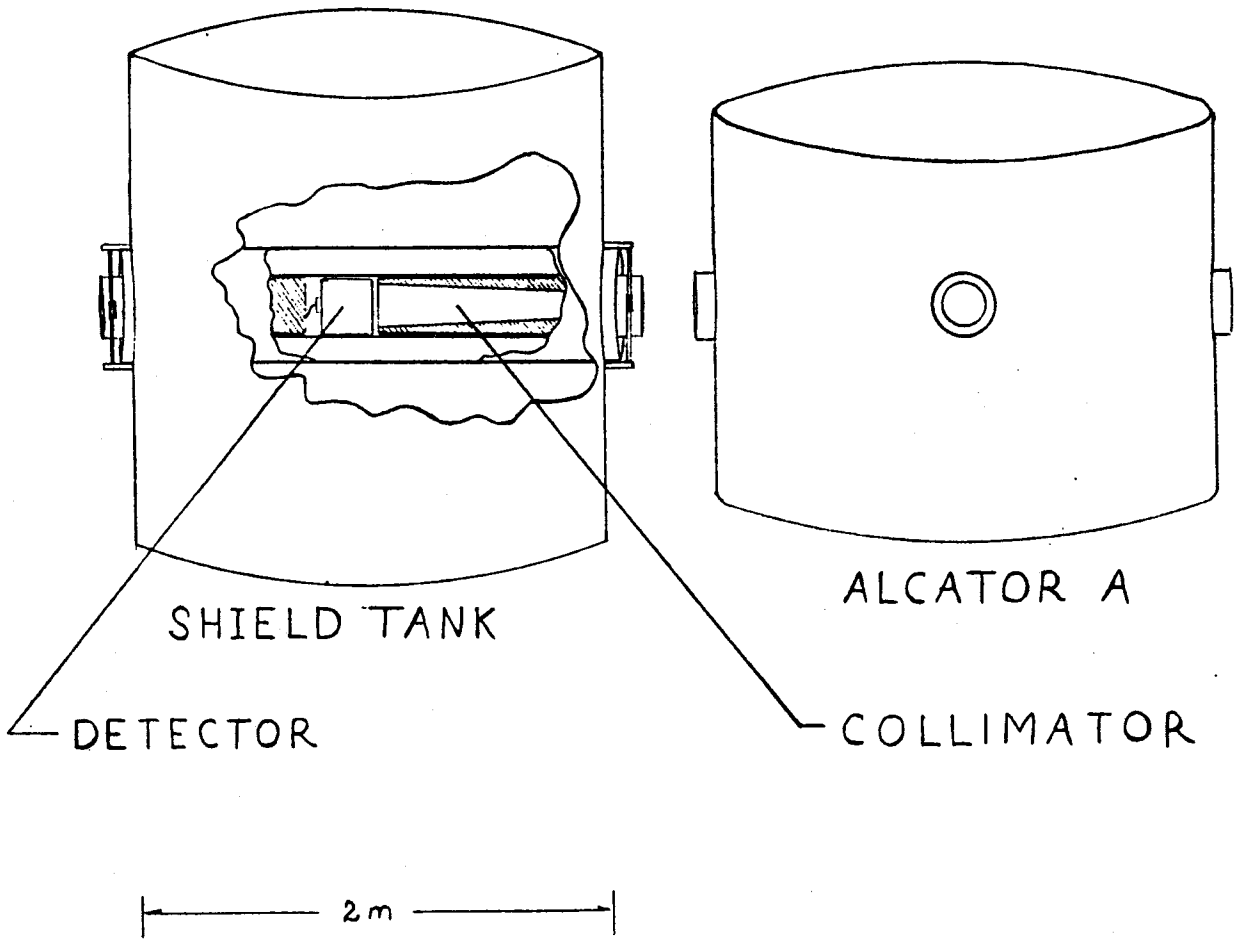

Figure 1.3 Experimental Set-Up of Alcator Collimator

evolve through the problem geometry. Tallies are kept on the total number of neutrons and their energy for any region of interest. The variance of the results is directly dependent on the number of neutrons involved in each tally. Thus,great care must be taken to make each neutron history contribute as much information as possible. For example, a full and complete Monte-Carlo simulation could involve very complex and detailed information of the system modeled. However, the resulting model could take a prohibitively long time to solve. Thus one wishes to use techniques to reduce computation time while maintaining solution accuracy. One example is the use of symmetry.

1.5 The ANDY Monte-Carlo Code

The "ANDY" Monte-Carlo code was chosen for this problem because it uses the standard "ANISN" format cross-section set and the code has had some previous use in the Department of Nuclear Engineering.[3]

1.5.1 Cross-Section Input

The ANDY code is a discrete-energy, multi-group code. The cross-section data is averaged over finite energy groups and yield probabilities of scattering from one group to another. The accuracy of energy resolution is constrained by the fineness of the energy groups.

The spatial or angular scattering information is contained in a Legendre expansion of the cross-section data to third order. Operationally in ANDY, scattering is always assumed isotropic in the laboratory system. The anisotropic nature of the scattering is obtained through the use of a weighting scheme. The neutron weight, set to unity at the start of the history is multiplied by $\sigma_{gg}'(\mu_o)/\sigma gg'$, where $\sigma_{gg}'(\mu_o)$ is the zero order expansion cross-section and σ_{gg}' is the true cross-section to third order. Particles scattered in directions favorable to the cross-sections are given higher weight. If the scattering is truely isotropic in the laboratory system, the weight will remain very nearly one and this scattering option is particuarly applicable.

1.5.2 Geometry

Geometry in ANDY is described through a three level topology. Regions are the highest level, bounded by surface segments, which are an intermediate level. The surface segments lie on surfaces, the lowest level. Any surface up to a second order quadraic can be modeled in the ANDY geometry coding. Surface segments are defined by the surface they lie on and by the surfaces which intersect them. A detailed example of ANDY geometry input is given in Appendix C.

CHAPTER 2. CODE DEVELOPMENT

2.1 Modeling Goals and Outline

The primary purpose of this thesis was to obtain a technique for modeling the Alcator A spatial collimator which would aid in the understanding of the collimator performance. In particular the following goals were set forth:

1. The modeling technique should be able to reproduce the experimentally determined point source response of the present Alcator collimator,

2. The modeling technique should be simple to modify for parameter studies, and

3. The modeling technique should be as economical of computer time as possible.

These goals were met by the development of the computer code, COLLUM.ANDY.

The COLLUM.ANDY code is a modified version of the ANDY Monte-Carlo code described in Chapter 1. No major modifications were required, the bulk of the work was in developing a standard input set for the collimator. The input deck development included:

1. Selection of a cross-section set,
2. Development of a geometry model,
3. Writing suitable SOURCE subroutines, and

4. The addition of some input variables and some code modification to obtain the point source response on a single run.

Each of these areas will be discussed in detail in this chapter. Test results will be presented in Chapter 3.

2.2 Cross-Section Set Selection

The cross-section set used for this modeling is a modified version of the Los Alamos LIB-IV cross--ection set. [4] The LIB IV set is a 50 energy group, 101 isotope set. In order to minimize storage and processing requirements the set was reduced to 20 energy groups and 8 isotopes.

In order to maintain the maximum information in the high energy groups, the lowest 30 groups were colasped to one and the upper 20 left intact. The energy structure is shown in Table 2.1.

The isotopes in the problem library set, "LACX3", include: Hydrogen, Boron^{10}, Boron^{11} , Carbon, Oxygen, Nitrodgen, Copper, and Cadmium.

As mentioned earlier the construction material of the collimator is plexiglass. The Composition of Plexiglass[(5)] is 8% Hydrogen, 32% Oxygen, and 60% Carbon, in weight percent. This corresponds to atom densities of 5.68×10^{22} atoms/cc Hydrogen,

GROUP	ENERGY RANGE (eV)		LETHARGY
01	1.5000E+07	1.0000E+07	0.692
02	1.0000E+07	6.0653E+06	0.5
03	6.0653E+06	3.6788E+08	0.5
04	3.6788E+06	2.2313E+05	0.5
05	2.2313E+06	1.3534E+06	0.5
06	1.3534E+06	8.2085E+05	0.5
07	8.2085E+05	4.9787E+05	0.5
08	4.9787E+05	3.8774E+05	0.25
09	3.8774E+05	3.0197E+05	0.25
10	3.0197E+05	2.3518E+05	0.25
11	2.3518E+05	1.8316E+05	0.25
12	1.8316E+05	1.4264E+05	0.25
13	1.4264E+05	1.1109E+05	0.25
14	1.1109E+05	8.6517E+04	0.25
15	8.6517E+04	6.7379E+04	0.25
16	6.7379E+04	5.2475E+04	0.25
17	5.2475E+04	4.0868E+04	0.25
18	4.0868E+04	3.1828E+04	0.25
19	3.1828E+04	2.4788E+04	0.25
20	2.4788E+04	1.00000E-05	23.81

TABLE 2.1 ENERGY GROUP STRUCTURE OF LACX3 CROSS-SECTION SET

1.42×10^{22} atoms/cc Oxygen, and 3.55×10^{22} atoms/cc Carbon. All material regions were modeled using this composition.

Non-material regions were modeled using a 1×10^{15} atom/cc density of Hydrogen.

2.3 Geometry Model

The Alcator collimator described in Section 1.3 and shown in Figure 1.2 has a complex geometry, containing 448 cells or regions. Representing this geometry in full detail using the ANDY geometry input scheme [3] would require about 30K bytes of core memory. Although 30K bytes is well within the capacity of the active core capacity of the IBM 370 machine (>1000K bytes) used, an input set of this size would be impracticable if the modeling technique were to meet the goal of ease of use in parameter studies.

In order to gain the simplification needed, the symmetry of the collimator was used. All of the 448 cells in the collimator are identical in dimension. Further, the centerline of each cell goes through a common point 122 cm in front of the collimator as in Figure 2.1. Thus, a point source at the common or focal point is viewed equally by all the cells. If the source is moved perpendicular to the central cell, it is not moving perpen-

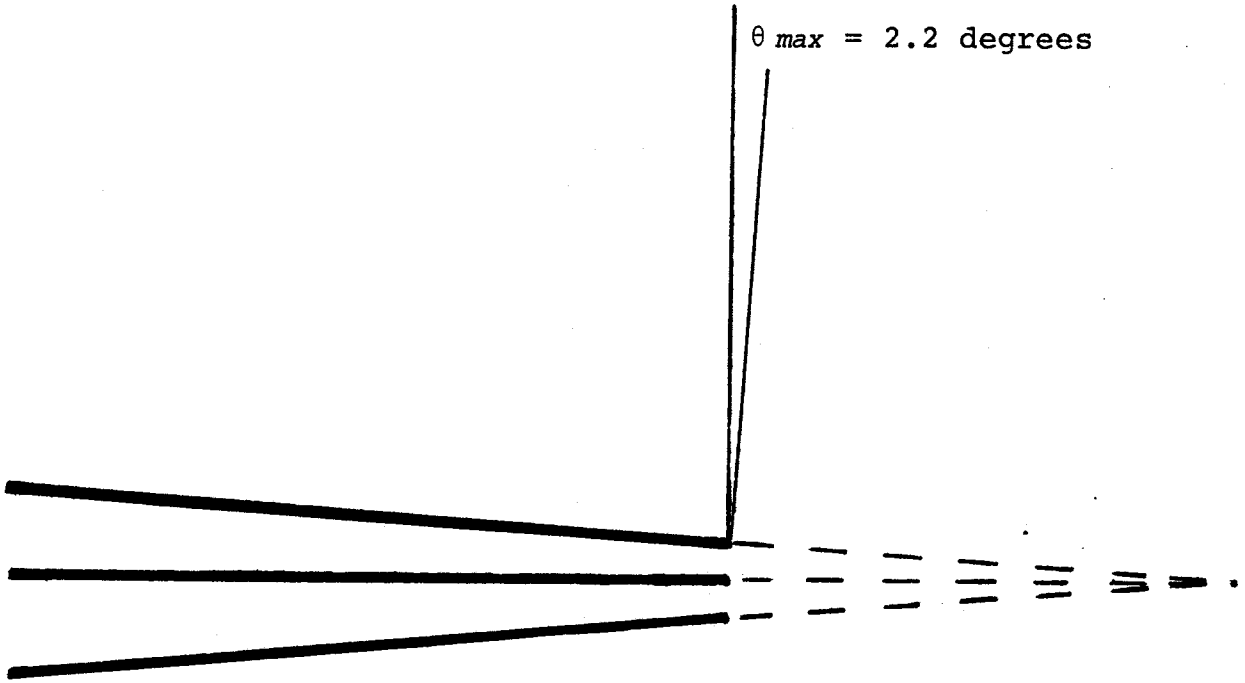

Figure 2.1 Symmetry of Collimator Cells

This is a simplified version of figure 1.2 showing an x-plane cut of the collimator. Only the center and edge cells are drawn.

dicular to the other collimator cells. However, the deviation is quite small, 2.2 degrees for the edge cells, resulting in an error of less than 0.08% in the path length. Thus, a single cell modeling, with the proper boundary conditions can provide the simplification needed.

The geometry model used is a single-cell with spatial reflecting walls shown in Figure 2.2. Although the neutron remains in a single cell in the computor simulation, the effect of the reflection condition is to form an infinite array model. Each reflection plane results in virtual cell opposite. Since reflection planes are in a sense reflected also, an infinite array results. Here, the term "virtual" means virtual in the computer model sense. A vertical cell in the computer model represents a real cell in the real collimator.

In the real collimator a major portion of neutrons interacting in the collimator leak out the sides. In order to model this effect, which is due to the finite extent of the collimator, a technique called "virtual cell tracking and cut-off" was developed. The technique is as follows. In the computer simulation a reflection indicates that the neutron would have entered an adjacent cell in the real collimator. This adjacent cell is virtual in the computer model sense as in Figure 2.2. Through coding logic, the virtual cell corresponding to a reflection or a series of reflections and collisions,

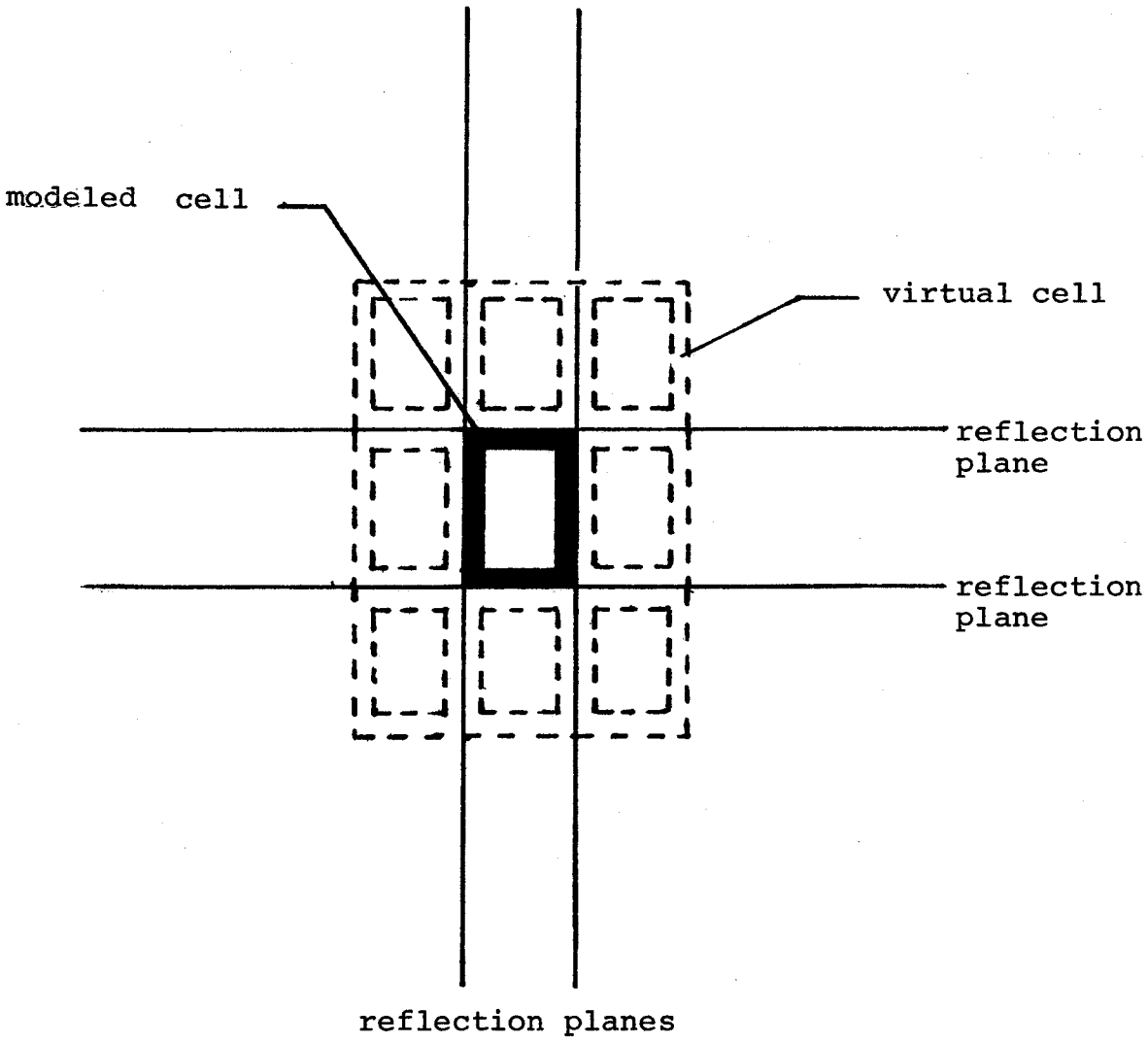

Figure 2.2 Infinite Array by Spatial Reflection
This represents a view along the z axis of figure 1.2.

is deduced. The finite nature of the real collimator is modeled by setting a number limit on how many virtual cells may be transversed relative to the initial starting cell, and terminating the neutron history if the limit is exceeded. For example, in Figure 2.3 the initial cell is the central cell in the finite array shown. The view is along the Z axis of the collimator. The path shown is a projection of the path in three dimensions onto the x-y plane. In this example, the neutron history reflects six times in the single cell of the computer simulation. The corresponding path traverses five virtual cells. Since a sixth virtual cell represents a real cell outside the finite extent of the real collimator, the history is terminated. Input parameters are used to specify the initial cell position and the number of cells. Thus, any initial cell in a finite collimator array of any size is modeled with only the geometry input for a single cell and a few additional parameters.

A tally is kept of the number of histories entering each virtual cell. This tally yields information on how the neutrons penetrate through the collimator.

2.4 Source Subroutines

Because of the general nature of ANDY, the "SOURCE" subroutine, which provide the initial position, direc-

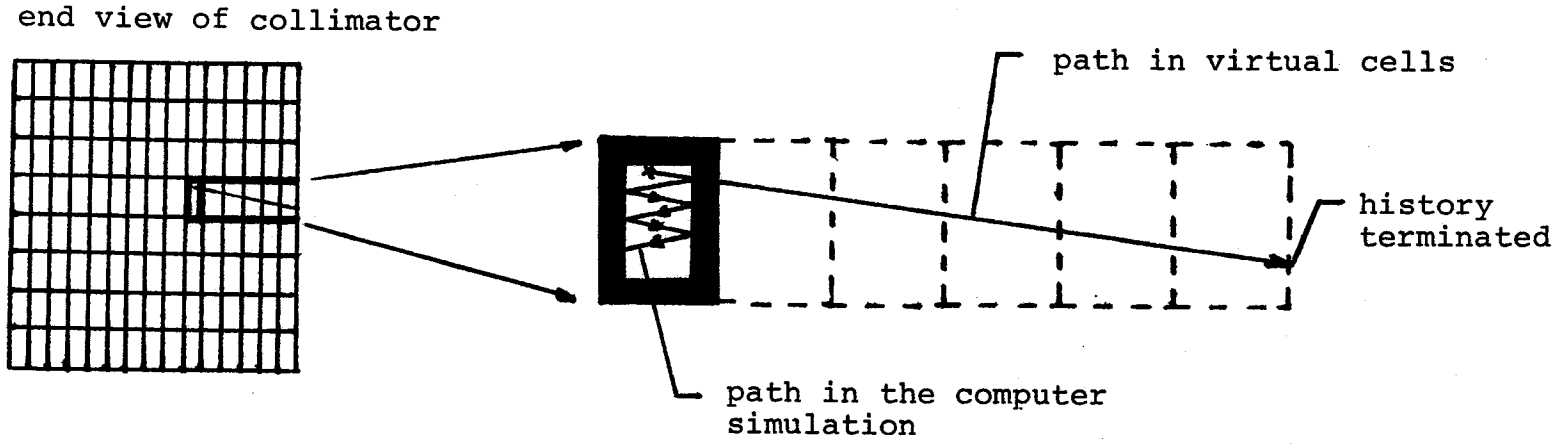

Figure 2.3 Virtual Cell Tracking

The path in the virtual cells represents the real path in the real collimator.

tion cosines, region, and energy group is not a standard part of ANDY coding. Thus each problem must provide a subroutine "SOURCE". In the ANDY Monte Carlo code, the SOURCE subroutine behaves as a distribution function which is sampled a fixed number of times. Each sampling is called a history, an ensemble of histories is called a trial. The primary requirement of the SOURCE subroutine is that the distribution of initial history values of the complete ensemble or trial reproduces the distribution of the real source. Two SOURCE subroutines have been developed. One subroutine uses a random sampling technique in choosing the initial variables, the second uses a fixed source distribution.

2.4.1 Fixed SOURCE Subroutine

In the Fixed SOURCE subroutine an ensemble of initial history values is built which reproduces the point source distribution. When the subroutine is called, the ensemble is sampled in a fixed sequence until all of the ensemble values have been used once. Thus, all of the initial variables of any history and for the trial as a whole is known. Figure 2.4 illustrates how the initial history variables are generated. Recall that only a single cell is modeled using the virtual tracking methods. Particles are given an initial Z value corresponding to

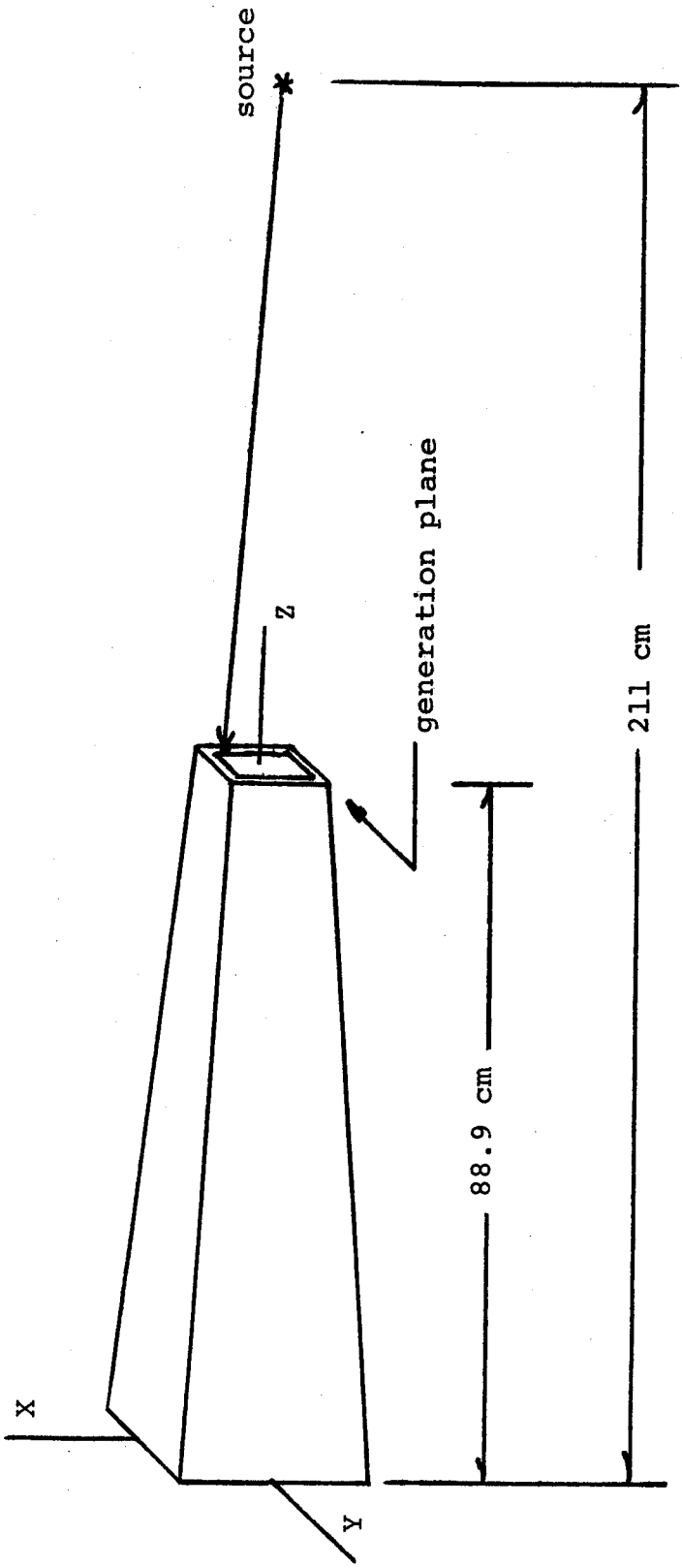

Figure 2.4 Initial Parameter Generation

the face of the collimator (Z = 88.9 here). The x and y values are then generated on this surface. Since the neutrons really begin at the source (Z = 211), the initial direction cosines are obtained by projecting a ray back to the source. Thus, a neutron history begins at the face of the collimator but is identical to a history which began at the source and arrived unscattered at the collimator face. This last assumption is valid for 2.5 Mev neutrons which have a mean free path of greater than 100 meters in air.

In the fixed source distribution subroutine the distribution of x and y are fixed at the center of square areas generated by a grid dividing the face of the collimator into equal areas as shown in Figure 2.5. The fineness of the grid is dependent on the number of neutrons histories to be following in the trial.

As in all Monte-Carlo codes, history rejections due operational limitatons of the computer and code occur; and must be subtracted from the trial results. In the ANDY code, which does all its random number generation internally, the rejected history is re-run with a negative weight. This requires that the SOURCE subroutine return the same initial values for a given random number seed.

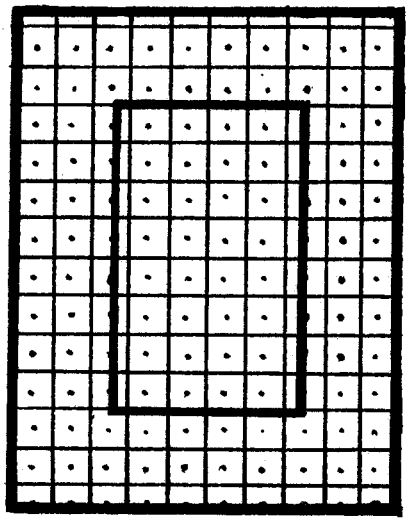

Figure 2.5 Grid Pattern for Fixed Source Distribution

Since the Fixed SOURCE subroutine did not use the seed for finding the initial values, a special set of instructions was designed to handle rejections. On the retracing call the "last call" values are returned. On the next call, which would be the history to replace the rejected history, the "last call" X-Y coordinate are returned with a perturbation of one-tenth of the fixed grid dimension added or subtracted to one of the coordinates. The selection of whether to add or subtract is govenered by whether the history number is odd or even and the coordinate selection is perpendicular to the direction last incremented. If the rejection occurs again the process is continued. If five consecutive rejections occur, the parallel coordinate is incremented. In all cases the old and new x-y values are printed so that a correction can be made to the distribution variance.

In addition to spatial coordinates and direction cosines, the initial region, energy group, and weight must be provided. The energy group and weight are simply assigned values of 4 and 1 respectfully. The initial region is found by a logic sorting section which uses input check-values XSET and YSET. Figure 2.6 shows the region structure used in the single cell model. The input variables X-set and Y-set are passed to SOURCE via

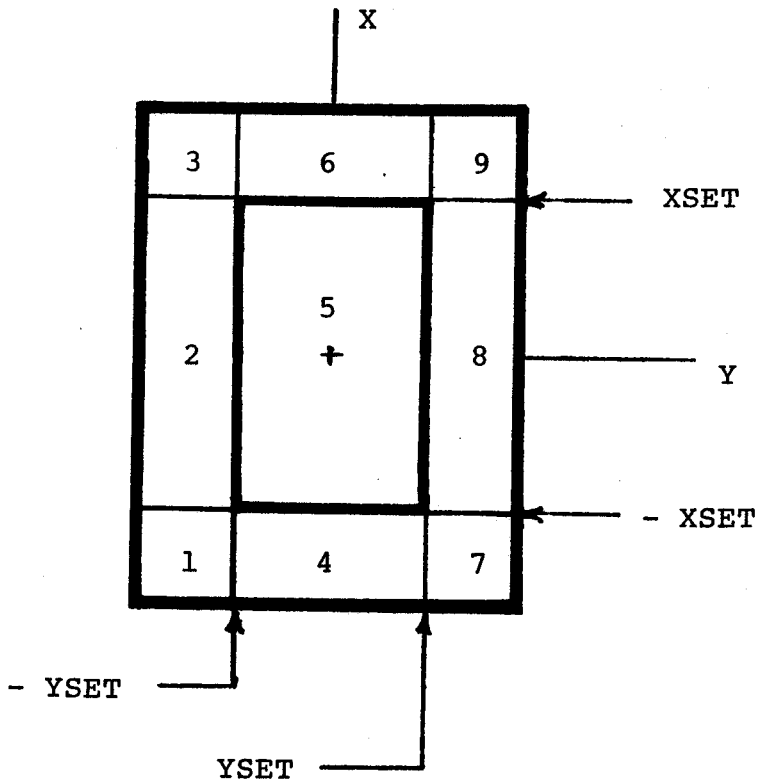

Figure 2.6 Regions of Single Cell

at a common block EXTRA.

2.4.2 Random SOURCE Subroutine

The Random SOURCE subroutine is completely interchangeable with the Fixed Source subroutine, i.e., no changes are needed in the input data, unneeded parameters are ignored. It differs from the fixed SOURCE subroutine only in that the x-y coordinate values are randomly generated on the face of the collimator.

Both SOURCE subroutines have been interfaced to the main processing routine BUSY so that a number of trials are performed with the position of the source incremented on each trial. The details of the input variables are included in Appendix D.

2.5 Code Modifications

A number of modifications were made to ANDY code, falling into three major areas:

1. Virtual cell tracking,
2. Shewed plane reflection, and
3. Point source scanning.

2.5.1 Virtual Cell Tracking

The modifications for virtual cell tracking involved;

1. Testing after each collision to correct the virtual track path sign flag,
2. Updating the virtual cell number each time

a reflection occurs, and

3. Tallying the number of histories entering each virtual cell and print-out of the tallies.

The test at each collision is simply a check to see if the sign of any of direction cosines had changed. A change in a direction cosine results in a change of the sign of a corresponding direction flag. For example, if a particle history had UX=0.5 before a collision and UX=-0.7 after, then the sign of the UX direction falg would change. This flag is used in the updating of the virtual cell number when the next relfection occurs. Reflections do not change the direction of the virtual path but collisions may.

The updating of the cell number involves incrementing or decrementing the appropriate cell number, depending on which boundary the relfection occurs at and the sign of the direction flag. For example, consider a history reflecting on an x-z plane and with the UY direction sign positive. The Y cell number would be incremented (Note: the planes are skewed planes in the actual model and appropriate steps are taken to correct for this effect).

When the cell number exceeds the number of cells in the collimator (an input parameter) the history is term-

inated. For example, in the Alcator modeling tests (Chapter 3) the number of x cells was set to 14 and the initial cell at the start of each particle history was 7. Histories which would have ended in cells 14 or 0 were terminated and tallied as escaped histories in the ANDY tallies.

The cell tallies are kept by incrementing the cell tally when a history enters the cell. As an example of how a cell tally is obtained, consider a 5 cell collimator in one direction. Assume that there are 5 histories and that they follow the following history paths;

History	Cell History
1	3 → 2 → 3 → 4 → X
2	3 → X
3	3 → 4 → 5 → X
4	3 → X
5	3 → 2 → 1 → 2 → 3 → 4 → 5 → X

where the X means the particle history ended either due to absorption, leaving the end of the collimator, or exceeding the cell parameters. The cell tally would yield:

ICELX(I) I=1, NXC where NXC=5 here

1 3 2 3 2

Since only the returning histories and not the initial histories in cell 3 are tallied, the tally value of cell

3 yields a form of an albedo.

2.5.2 Shewed Plane Reflection

The coding to handle reflections from the x-z and y-z shewed planes used to model the Alcator collimator had to be written. Reflections are assumed to be specular, and the modifications were straight-forward. Further details can be found in the code listing, Appendix E, lines 824 through 846.

2.5.3 Point Source Scans

In order to reduce the duplication of set up procedures, the code was modified to do a preprogrammed number of trials incrementing the source position in the y-direction. This modification was only involved in the writing of the SOURCE subroutine since ANDY already had a multi-trial option. In SOURCE, a set of conditions is checked, in particular, the history number. When the source position is incremented, its new value is printed as can be observed in the output in Appendix B. The number of trials is controlled by input parameters.

A number of input parameters have been added to the ANDY input parameters. Appendix D is a guide to all the COLLUM . ANDY input parameters.

CHAPTER 3. MODELING RESULTS

Three modeling comparisons and one experimental comparison are discussed in this chapter.

First, the base case from which the final Alcator collimator modeling results were obtained, is discussed.

Next, three comparisons to this base case are made in the following areas; an infinite cell model in which virtual cell tracking has not been used, an edge test in which a cell near the edge is modeled, and a test of the Fixed SOURCE subroutine. Finally, a comparison of the basic case to the experimental results is presented.

3.1 Alcator Modeling Base Case, Test A

The COLLUM.ANDY output has three major parts; an abbreviated history trace, surface tallies of history weight, and the virtual tracking cell tallies. The history trace consists of a detailed account of the first ten boundary crossings, reflections, and collisions. This section of output provides a very useful tool for verifying the correct operation of the code. Appendix B contains detailed output.

The tallies of history weight reaching specified surfaces or surface tallies, are the major source of information in the code. Recall from Chapter 2, Figure 2.6 that the single cell is composed of nine regions.

In addition 10 surfaces and 42 surface segments were needed to model the single cell. Only one of the 42 surface segments needed to be tallied for this problem. Other surface sements were tallied for operational and checking purposes. Here, only the tally of the surface segment corresponding to the back end and middle region (region 5 in figure 2.6) is presented.

Figure 3.1 is a histogram plot of history weight as a function of source position for energy groups 4, 5, and 6. Each trial has 1058 histories generated by the random source distribution. A typical error bar is shown for source position 0.2cm and group 4. Note that essentially no histories are obtained in energy groups 5 and 6 indicating that only non-collisional histories or histories scattered through very small angles contribute to the tally. Further, the history tally drops in group 4 when the source is greater than 0.4cm off center indicating a cut-off or the collimator resolution. Recall from Chapter 1 that a perfectly absorbing collimator would have a cut-off at about 0.46cm. Further analysis of the collimator resolution is presented in the experimental comparison, Section 3.5. The third part of the output is the virtual cell tracking cell tally. Table 3.1 lists the cell tally in the x and y direction for the center-line source positions, 0.0 cm.

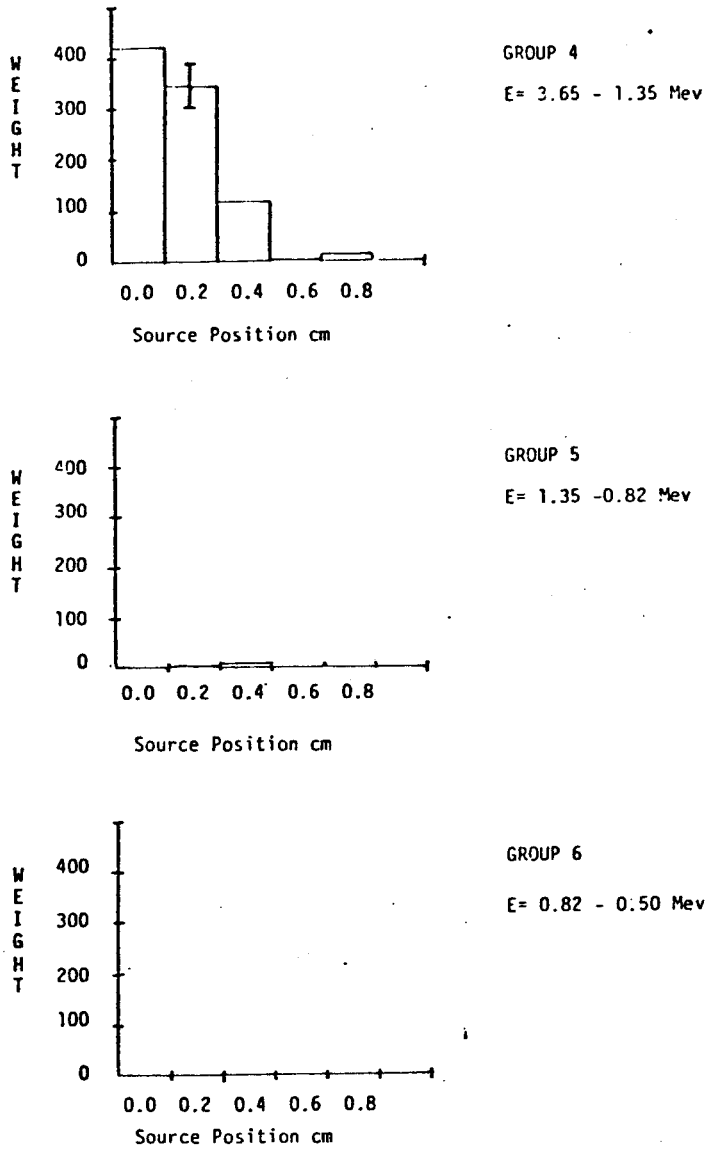

Figure 3.1 COLLUM.ANDY Surface Tallies by Energy Group and Source Position

ICELX(I) I=1, NXC									
101	129	180	250	335	451	218	470	357	274
204	144	100	70						
ICELY(I) I=1, NYC									
66	72	87	98	108	119	141	164	195	229
263	292	337	384	476	214	508	435	370	314
276	235	213	193	169	155	138	119	100	79

TABLE 3.1 Cell Tally for 0.0cm Source Position

Histories were started in X cell 7 and Y cell 16. X cell 1, Y cell 1, X cell 14, and Y cell 34 correspond to the model edges. NCX and NCY are the number of X cells and Y cells and are equal to 14 and 32 respectfully. As can be seen from the table, more than 10% of the histories reach the edge of the collimator. It should be noted that these are number tallies and do not reflect the anisotropic nature of the cross-sections. However, the tallies do serve as a guide in determining how strong the intercell interactions are. The strength of the intercell interactions is explored in more detail in the edge test comparison, Section 3.3.

Execution time for one trial of 1058 histories is about 28 seconds. Comparison tests indicate that

the variance in execution time due to IBM-370 operating system may be as high as 6%.[6] Under the 'DEFER' option with a shift factor of 0.6 times the true cost; a typical trial costs about $3.60 plus printing costs. Set up time costs for the initial part of the code appear to be negligible.

3.2 Infinite Cell Test B

One type of model often used in this type of simulation is an infinite cell model. The COLLUM.ANDY uses the infinite cell technique but improves upon it through the use of virtual cell tracking. It turns out that the main improvement is in execution time.

The infinite cell test involved running the base case collimator with the virtual cell tracking and cell cut off eliminated resulting in the infinite collimator described in Chapter 2.

Source Scan Position (cm)	Test A	Test B	Test X
0.0	448	412	414
0.2	314	337	334
0.4	123	125	117
0.6	1	---	2
		Standard deviation ∿32	

TABLE 3.2 Surface Tally Wieghts For The Infinite Cell Case. Test A-base case Test B-infinite cell, Test X-Test A run with different random number sequence. The group tally weight is a sum of energy groups 4, 5, and 6.

While the tally results for surface segment tallies agreed within a standard deviation, Table 3.2 (in fact a previous run with a different random number had given perfect agreement) the infinite cell test required almost twice as much CPU time. The base case required 28.5 seconds per trial and the infinite cell test 54.3 seconds per trial of 1058 histories. This represents a major savings in computer costs.

3.3 Edge Tests C and D

In the infinite cell test the actual surface segment tallies represent the histories that would be seen by a detector in the real world,were found to be insensitive to whether the collimator was finite of infinite. This was found to be true for the edge tests also.

Because the source scan is done only on one half of the collimator, two tests on opposite sides of the collimator as in Figure 3.2 are needed to eliminate the non-sysmetric effects. The initial cell was set to 31 for test C and set to 2 for test D. Table 3.3 summarizes the surface segment weight tallies for all tests considered thus far. It also includes a test E, a fixed source distribution test to be considered in the next section.

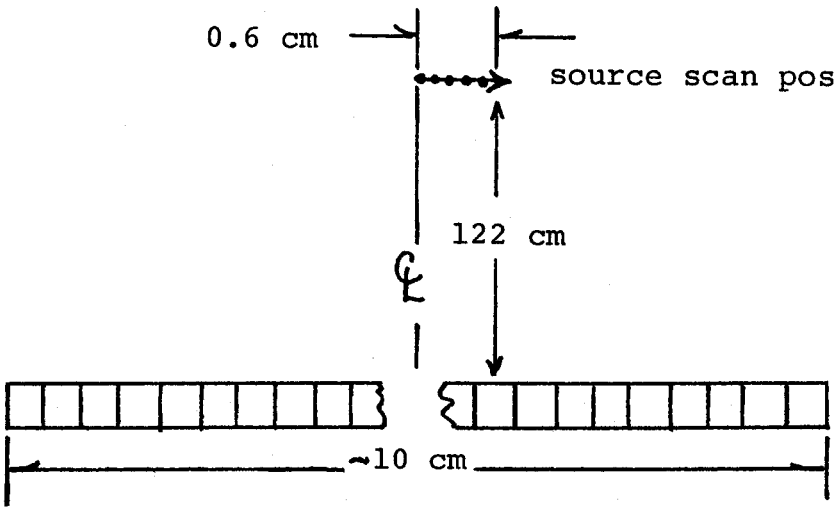

Figure 3.2. Edge Test Layout

Source Scan Position (cm)	Test A	B	C	D	X	E
0.0	448	412	405	414	414	398
0.2	314	337	298	296	334	304
0.4	123	125	118	113	117	104
0.6	1	--	6	4	2	3

Table 3.3 Surface Weight Tallies for Edge Tests

Non-symetric effects are not apparent in Table 3.3 for Tests C and D. For the 0.0cm source position the source is still in a symetric position and the two values fall within a standard deviation of each other. For the skewed source positions, 0.2cm - 0.6cm, there is essentially no difference. Further, these edge cell

weight tallies agree well with the previous tests.

This agreement implies that the intercell interactions are not a significant factor. This is due to the length of the collimator. As was explained in the introduction, a neutron must go through 10 mean free paths to reach the detector end of the collimator. Since the plexiglas construction material is so high in Hydrogen the neutrons are moderated below the cut-off energy (32 Kev) before they reach the end of the collimator. Thus, most of the weight at the detector end of the collimator is due to unscattered histories and collimator appears essentially black to bad geometry neutrons. If the collimator were shorter or made of a less efficient moderator, scattering effects could become significant.

While the weight tallies were unchanged, execution time differed greatly for tests C and D. Test D required only 5.25 seconds CPU time per trial while Test C required 25.5 seconds CPU time per trial. Test D corresponds to histories which had short paths as the source was scanned and thus were very short histories. The skewing can be seen in Table 3.4 which gives the y direction cell tallies for tests C and D at source position 0.6cm.

ICELY(I) I=1, NYC				for Test C					
60	67	84	90	109	126	140	144	160	174
184	195	210	227	251	277	300	340	385	435
477	514	588	671	759	840	939	1067	1224	1400
289	249								
ICELY(I) I=1 NYC				for Test D					
995	0	0	0	0	all other entries are zero				

Table 3.4 Edge Tests Cell Tallies

3.4 Fixed Source Distribution, Test E

Test E uses the base case but uses a fixed source distribution as described in Chapter 2. Table 3.3 presented in the previous section, summarizes the results of the fixed source distribution test. Unlike previous tests, the results appear to be systematically lower. Because the fixed source distribution is known a more detailed analysis is possible.

A collimator cell presents non-material and material (the cell wall) paths for a neutron history. If the walls were perfectly black a ratio of the cross-sectional areas at the face of the collimator would give the transmission for the source position at 0cm as 0.375 or 397 histories. 374 of the 1058 trial histories were started in the non-material region. Thus, if the walls were perfectly black,

the Fixed Source test would underestimate by 23 histories simply due to how the initial starting positions were chosen. This is roughly the discrepancy seen in Table 3.3. The reason for the discrepancy is due to the fact that the distribution grid was set up poorly. The grid pattern lies such that a small change in the position of a row will take the whole row of histories from across a material to a non-material boundary. Thus the technique is very sensitive to source grid selection. Although it was not done in this thesis a possible solution is to use a grid skewed to the material boundary. Operationally this type of grid is more difficult to develop and use but should eliminate the systematic error of the present fixed source grid. This example indicates that great care must be taken to avoid systematic error when a fixed distribution is used.

If 396 histories are predicted for a perfect absorber case, why is the average value in the tests around 418? There are two possible causes.

The first is simply additional transmission and scatter. While the collimator cells expands to about 4 times in cross-sectional area from front to back, the wall thickness is constant. Since the mean free path of the energy group 4 neutrons is on the order of 5cm some additional neutrons go through the wall as shown in Figure 3.3.

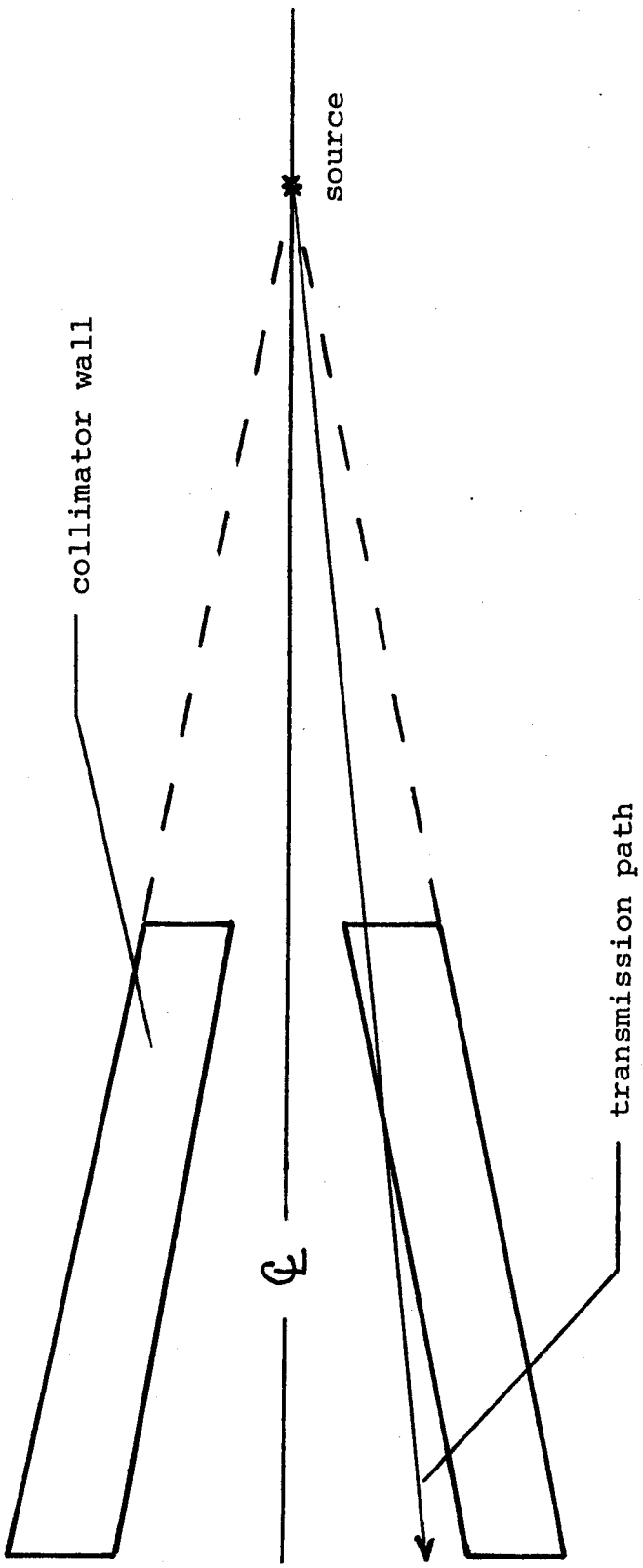

Figure 3.3 Transmission Through Collimator Walls

Using the area argument again one would expect 246 histories to have paths which could pass through the wall. Of the 246 only about 20 have material path lengths less than one mean free path. One would expect 10 of these 20 to pass through the material without a collision. If the 2 and 3 mean free path histories are added the total histories would be around 15. Further small angle scacttering can add to the number obtained. Scattering at less than 10 degrees will not change the energy group even for hydrogen scattering. For isotropic scattering, no second scattering,and for scattering occurring in the first 3 mean free paths of the collimator, the scattering sources can be considered as a point source located roughly 3/4 of length of the collimator from the detector end. At this distance the entire collimator subtends .0036 of the total solid angle. 680 of the 1058 histories started can scatter so 0.0036 times 680 or 215 histories are estimated. Thus, transmission and scattering, in an order of magnitude estimate, accounts for the discrepancy from the perfect absorber case.

The second source of error is a systematic error due to the random source subroutine and operational characteristics of the code. In the random source subroutine the initial distribution is randomly generated

on the face of the collimator. This gives this technique an advantage over the fixed distribution which at present is very sensitive to how the grid is chosen. However, a bias can occur in the random distribution because operational errors are rejected in the code logic. Qualitatively, histories which spend more time in the processing of the code stand a higher chance of rejection. Since the random source generates randomly there is a bias for short histories. Histories which do not scatter take less time, so some bias might be expected in the forward direction resulting in higher weight tallies. The fixed source technique does not suffer from this problem because it maintains roughly the same distribution. On a rejection the next history is only slightly perturbed from the rejected path.

It is possible to set an upper bound since the number of rejections in a trial is a known parameter. In the base case for example for the 0.0cm source position 37 rejections occurred. Assuming the replacement histories are randomly generated 0.318 times 37 or 12 histories may be bias to non-material regions. Thus the bias appears to be small but could be significant. Thus, an improved fixed source distribution may be justified if a larger number of histories per trial are used. At

present with 1058 histories per trial the variance in source generation is 32.5, or about 3%.

3.5 Experimental Results Comparison

The point source response of the Alcator collimator was measured using a ^{252}Cf neutron source. The average neutron energy is 2.35 Mev. The source was located 122cm in front of the collimator and was essentially a point source. The data from the experiment and from Test X (Test X had 10 data points in the scan rather than 4 as in Test A, the base case) were fitted using a cubic spline fitting routine.[7] Figure 3.4 shows the results. Figure 3.5 shows the experimental points on the computer generated curve. The error bars shown are typical. The fwhm for the experimental result is 7.2mm and the fwhm for the computer simulation is 7.0mm which is in excellent agreement. Disagreement between the two in the wings occurs because of back-scatter effects in the experimental results. The results of ANISN calculations[8] indicate that back-scattering of neutrons from the walls in a room could add as much as 5% to the source response. The fall-off seen seems to agree with this analysis. The negative value of the computer simulation curve is an artifact of the cubic spline fit.

Figure 3.4 Cubic Spline Fits to Computer Simulation and Experimental Results

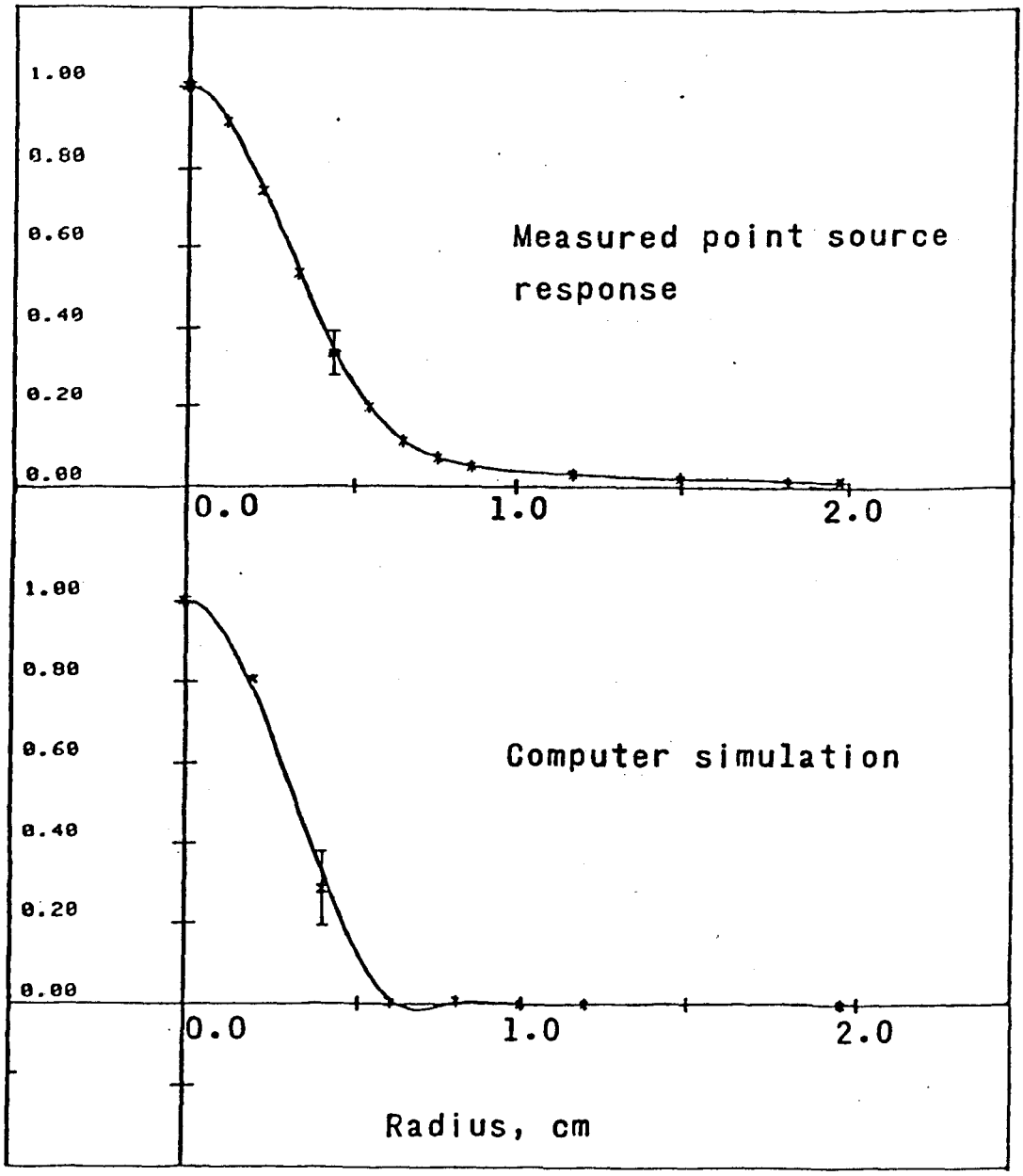

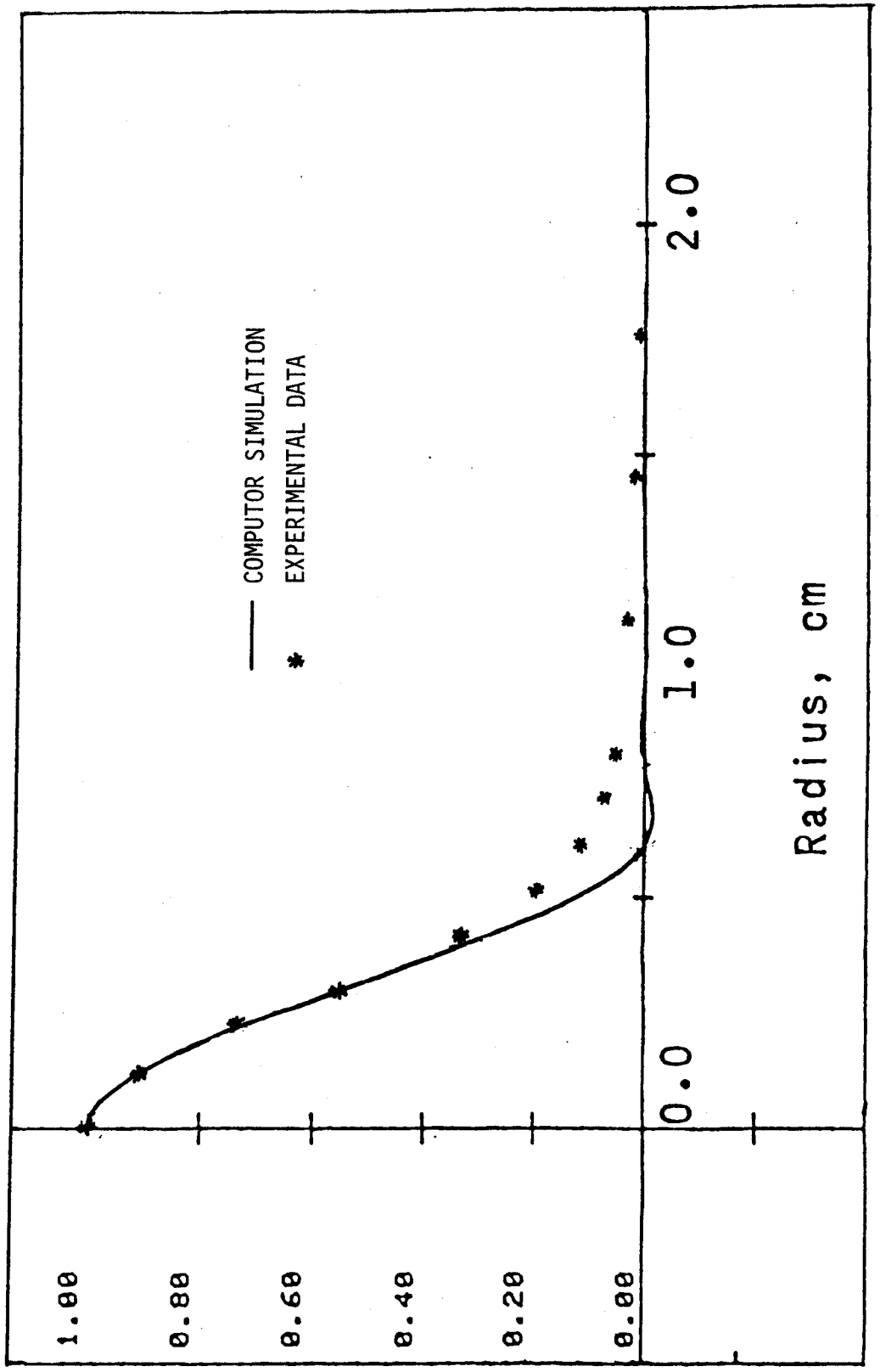

Figure 3.5 Comparison of Experimental Data Points and Computer Simulation Curve

CHAPTER 4. SUMMARY AND CONCLUSIONS

4.1 Modelling Goals

The COLLUM.ANDY code has met the goals set forth for the collimator model in Chapter 2.

The code has reproduced the point source response of the Alcator collimator as was seen in Figure 3.3.

The code is easy to modify allowing parametric studies to be done easily. For example, the virtual cell tracking and cell cut-off technique allows one to change the number of cells in the collimator and the particular cell to be modeled through the change of just 4 input parameters. Thus, edge cell analysis does not require a new geometry set. The virtual tracking method was described in Section 2.5. The versatility of the code is indicated in the model tests of Chapter 3. With the exception of the infinite cell tests, the base case required only one or two parameter changes to model very different conditions. In addition the virtual cell tracking cell tally yields additional insight on the physics of the collimator. For example, edge effects, which will become important if a shorter collimator is modeled, can be studied in more detail and with minor parameter changes.

The code proved to be economical of computer time. In particular, the COLLUM.ANDY code cuts the CPU time by

a factor of two when compared to an infinite cell model using the original ANDY Monte-Carlo code. This comparison was done in Section 3.2.

4.2 Collimator Performance

Although specific analysis of the collimator was not the purpose of this thesis, the analysis done here seems to support the design decisions. In particular, it is clear that if the collimator is long compared to a mean free path, ($L \geq 10$ mean free paths) the collimator will act as if it is a perfect absorber. Further, when the length condition is met, edge effects are minimal so correction is not needed for the edge cells. Sections 3.3 and 3.5 indicate these conclusions.

4.3 Future Work

Although the final model does a good job there are areas in which future work should be pursued.

The Fixed Source subroutine could be improved as was mentioned in Section 3.4.

The virtual cell tallies could be modified to give the weight rather than a number tally for each cell. This was discussed in Section 3.1.

Finally, the cross-section set and input parameters could be expanded to include a mixed neutron gamma ray set. This modification would allow both the neutron and gamma ray properties of the collimator to be studied.

REFERENCES

1. David Gwinn, Francis Bitter National Magnet Laboratory, Alcator Group, M.I.T., private communication.

2. Meyerhof, Elements of Nuclear Physics, McGraw Hill Pub. Co., N.Y.N.Y., 1975.

3. Multi-Group Monte Carlo Simulation of Neutral Particle Transport--A Users Guide to ANDY by Owen L. Deutsch - unpublished MIT N.E.D. report.

4. LIB IV, A Library of Group Constants for Nuclear Reactor Calculations, R.B. Kidman, R.E. MacFarlane, LASL Report, LA-6260-MS.

5. Paul Dunion of the Dupont Corporation, private communication.

6. Arthur Anger, M.I.T., Information Processing Services, Personal Communication.

7. "Plot 50 - Mathematics," Vol. 2, Tektronix 4051 Program Library, Tektronix, Inc., Beaverton OR.

8. D. Gwinn, Francis Bitter National Magnet Laboratory, Alcator Group, private communication.

APPENDIX A. ANDY HIERARCHY

Processing in ANDY follows a very straight-forward order. The main program begins by reading and processing input data on the complexity of geometry, number and type of cross-sections and types and number of tallies required. From this input the size of operational and storage arrays is calculated.

MAIN then calls subroutine "CXINP" if any cross-sections are to be read from the input deck. Next MAIN call subroutine "PREP". PREP reads cross-sections from tape or disk, the geometry input deck, and the material mixture and density input data for each region. PREP does a geometry consistency check, and mixes the macroscopic transport property tables for each mixture.

At this point, data input and problem set-up is complete and control returns to MAIN. MAIN then calls subroutine "BUSY", the main processing routine. The program ends upon return from BUSY. BUSY first initializes all tally bins to zero and then calls subroutine "SOURCE", providing it with a random number seed.

Subroutine SOURCE is not a standard part of ANDY coding and must be written for each problem. The purpose of the SOURCE subroutine is to provide the initial spatial coordinates, direction cosines, initial energy

group, and weight using the given random number seed.

BUSY uses this information to begin a particle history. Operationally, BUSY calculates whether a collision occurs before a boundary is reached by comparing a randomly generated collision distance based on the mean free path data to the boundary distance. In the case of a collision, BUSY branches to scattering, fission, or delayed particle emission logic. These sections modify the direction cosines, particle energy, or initiate a delay particle bank as reflected in the cross-section data. In the case of a boundary, BUSY tallies the boundary crossing, modifies the region, and cycles back to the collision check logic. The history is terminated when the particle enters a region outside the geometry, when the particle weight falls below a weight cut-off; or when operational error occurs. In the case of cut-offs, the particles weights are tallied. When an operational error occurs, the history is retraced and expunged.

Once a single particle history is complete, BUSY again calls the SOURCE subroutine and repeats the above sequence. When the prescribed number of histories have been completed, BUSY normalizes the tally arrays and prints the results.

ANDY output consists of a print-out of input variables with headings, an optional print-out of the processed cross-sections, an optional print-out of the history traces, and the print-out of number and weight tallies for each energy group, for each region or surface segment selected. Appendix B has a typical output for a COLLUM.ANDY run.

APPENDIX B. COLLUM. ANDY OUTPUT

ANDY TEST PROGRAM 4B ALCATCR COLLIMATCR

DATA

NG	NP	NING	NSCAT	NMIX	NLIBSM	NTPDEL	MCR	MTP
20	23	4	3	2	0	0	0	3

NBEG	NSUR	NSEG	NSEGRA	NSENMA
9	10	42	6	4

MT	ITB1	NTALB	NTALSS	NIT	NMATMA	NSUM
1	1	0	2	0	3	0

IUK	IGCUT	NG1	ICT	NSYMS	XNF
0	14	20	0	4	0.1058E+04

NXB	NYB	BD
46	23	0.138037E-01

NXC	NYC	NCEX	NCEY	XSET	YSET	YSP	YSINC
12	30	6	15	0.238137E+00	0.793733E-01	-.200000E+00	0.200000E+00

VARIABLE STORAGE ARRAY POSITIONS

LCHID	LDEN	LCL	LWIR	LWISN	LWISP	LHISP	LHISN	LDENSM	LCSUM	LDELPC	LWIT
1	2	8	468	469	510	551	592	633	634	635	636

KWIR	KWISN	KWISP	JWIP	JWISN	JWISP
637	638	679	720	721	762

LOCINI	LENGIA	LOCINA	LENGA
451	4000	4163	25000

STORAGE ALLOCATION ENABLES CORE RESIDENCE FOR 2MIXTURES

NS	NKRN	NORE	NPUNCH	NCOL	NDEV	NCRX	ISTPRT	NCPPRT
1058	3413	0	0	500	0	0	0	0

DELT1	DELT2	OFFSET	TSPLT	WDELP
0.100000E+09	0.100000E+09	0.100000E+09	0.0	0.0

DIMAX	WCOI	WSPLT
0.500000E+02	0.600000E-02	0.100000E+02

SURFACE NUMBER 1 OF TYPE 9	AS=-1.0807E-01	BS= 0.0	CS= 1.0000E+00	DS=-1.3021E-03	
	ES= 0.0	FS= 0.0	GS= 0.0		
SURFACE NUMBER 2 OF TYPE 9	AS=-7.6823E-02	BS= 0.0	CS= 1.0000E+00	DS=-1.3021E-03	
	ES= 0.0	FS= 0.0	GS= 0.0		
SURFACE NUMBER 3 OF TYPE 9	AS= 7.6823E-02	BS= 0.0	CS= 1.0000E+00	DS= 1.3021E-03	
	ES= 0.0	FS= 0.0	GS= 0.0		
SURFACE NUMBER 4 OF TYPE 9	AS= 1.0807E-01	BS= 0.0	CS= 1.0000E+00	DS= 1.3021E-03	
	ES= 0.0	FS= 0.0	GS= 0.0		
SURFACE NUMBER 5 OF TYPE 9	AS=-2.1615E-01	BS= 1.0000E+00	CS= 0.0	DS=-2.6042E-03	
	ES= 0.0	FS= 0.0	GS= 0.0		
SURFACE NUMBER 6 OF TYPE 9	AS=-1.8490E-01	BS= 1.0000E+00	CS= 0.0	DS=-2.6042E-03	
	ES= 0.0	FS= 0.0	GS= 0.0		
SURFACE NUMBER 7 OF TYPE 9	AS= 1.8490E-01	BS= 1.0000E+00	CS= 0.0	DS= 2.6042E-03	
	ES= 0.0	FS= 0.0	GS= 0.0		

```
 SURFACE NUMBER    8 OF TYPE  9   AS= 2.1615E-01   BS= 1.0000E+00   CS= 0.0          DS= 2.6042E-03
                                   ES= 0.0          FS= 0.0          GS= 0.0

 SURFACE NUMBER    9 OF TYPE  3   AS= 0.0          BS= 0.0          CS= 0.0          DS= 0.0

 SURFACE NUMBER   10 OF TYPE  3   AS= 3.5000E+01   BS= 0.0          CS= 0.0          DS= 0.0

 SURFACE SEGMENT NUMBER    1 IS IN SURFACE    1 WITH  4 SENSES
5       -6         9       -10

 SURFACE SEGMENT NUMBER    2 IS IN SURFACE    1 WITH  4 SENSES
6       -7         9       -10

 SURFACE SEGMENT NUMBER    3 IS IN SURFACE    1 WITH  4 SENSES
7       -8         9       -10

 SURFACE SEGMENT NUMBER    4 IS IN SURFACE    2 WITH  4 SENSES
5       -6         9       -10

 SURFACE SEGMENT NUMBER    5 IS IN SURFACE    2 WITH  4 SENSES
6       -7         9       -10

 SURFACE SEGMENT NUMBER    6 IS IN SURFACE    2 WITH  4 SENSES
7       -8         9       -10

 SURFACE SEGMENT NUMBER    7 IS IN SURFACE    3 WITH  4 SENSES
5       -6         9       -10

 SURFACE SEGMENT NUMBER    8 IS IN SURFACE    3 WITH  4 SENSES
6       -7         9       -10

 SURFACE SEGMENT NUMBER    9 IS IN SURFACE    3 WITH  4 SENSES
7       -8         9       -10

 SURFACE SEGMENT NUMBER   10 IS IN SURFACE    4 WITH  4 SENSES
5       -6         9       -10

 SURFACE SEGMENT NUMBER   11 IS IN SURFACE    4 WITH  4 SENSES
6       -7         9       -10

 SURFACE SEGMENT NUMBER   12 IS IN SURFACE    4 WITH  4 SENSES
7       -8         9       -10

 SURFACE SEGMENT NUMBER   13 IS IN SURFACE    5 WITH  4 SENSES
1       -2         9       -10

 SURFACE SEGMENT NUMBER   14 IS IN SURFACE    5 WITH  4 SENSES
2       -3         9       -10

 SURFACE SEGMENT NUMBER   15 IS IN SURFACE    5 WITH  4 SENSES
3       -4         9       -10

 SURFACE SEGMENT NUMBER   16 IS IN SURFACE    6 WITH  4 SENSES
1       -2         9       -10
```

```
  SURFACE SEGMENT NUMBER  17 IS IN SURFACE   6 WITH  4 SENSES
2       -3        9      -10

  SURFACE SEGMENT NUMBER  18 IS IN SURFACE   6 WITH  4 SENSES
3       -4        9      -10

  SURFACE SEGMENT NUMBER  19 IS IN SURFACE   7 WITH  4 SENSES
1       -2        9      -10

  SURFACE SEGMENT NUMBER  20 IS IN SURFACE   7 WITH  4 SENSES
2       -3        9      -10

  SURFACE SEGMENT NUMBER  21 IS IN SURFACE   7 WITH  4 SENSES
3       -4        9      -10

  SURFACE SEGMENT NUMBER  22 IS IN SURFACE   8 WITH  4 SENSES
1       -2        9      -10

  SURFACE SEGMENT NUMBER  23 IS IN SURFACE   8 WITH  4 SENSES
2       -3        9      -10

  SURFACE SEGMENT NUMBER  24 IS IN SURFACE   8 WITH  4 SENSES
3       -4        9      -10

  SURFACE SEGMENT NUMBER  25 IS IN SURFACE   9 WITH  4 SENSES
1       -2        5      -6

  SURFACE SEGMENT NUMBER  26 IS IN SURFACE   9 WITH  4 SENSES
1       -2        6      -7

  SURFACE SEGMENT NUMBER  27 IS IN SURFACE   9 WITH  4 SENSES
1       -2        7      -8

  SURFACE SEGMENT NUMBER  28 IS IN SURFACE   9 WITH  4 SENSES
2       -3        5      -6

  SURFACE SEGMENT NUMBER  29 IS IN SURFACE   9 WITH  4 SENSES
2       -3        6      -7

  SURFACE SEGMENT NUMBER  30 IS IN SURFACE   9 WITH  4 SENSES
2       -3        7      -8

  SURFACE SEGMENT NUMBER  31 IS IN SURFACE   9 WITH  4 SENSES
3       -4        5      -6

  SURFACE SEGMENT NUMBER  32 IS IN SURFACE   9 WITH  4 SENSES
3       -4        6      -7

  SURFACE SEGMENT NUMBER  33 IS IN SURFACE   9 WITH  4 SENSES
3       -4        7      -8

  SURFACE SEGMENT NUMBER  34 IS IN SURFACE  10 WITH  4 SENSES
1       -2        5      -6

  SURFACE SEGMENT NUMBER  35 IS IN SURFACE  10 WITH  4 SENSES
```

```
 1       -2        6       -7

  SURFACE SEGMENT NUMBER  36 IS IN SURFACE  10 WITH  4 SENSES
 1       -2        7       -8

  SURFACE SEGMENT NUMBER  37 IS IN SURFACE  10 WITH  4 SENSES
 2       -3        5       -6

  SURFACE SEGMENT NUMBER  38 IS IN SURFACE  10 WITH  4 SENSES
 2       -3        6       -7

  SURFACE SEGMENT NUMBER  39 IS IN SURFACE  10 WITH  4 SENSES
 2       -3        7       -8

  SURFACE SEGMENT NUMBER  40 IS IN SURFACE  10 WITH  4 SENSES
 3       -4        5       -6

  SURFACE SEGMENT NUMBER  41 IS IN SURFACE  10 WITH  4 SENSES
 3       -4        6       -7

  SURFACE SEGMENT NUMBER  42 IS IN SURFACE  10 WITH  4 SENSES
 3       -4        7       -8
  REGION NUMBER IR =  1     NAS =  6    IMIX =  1     IMPORT =        1     WCO =  0.600E-02    DNF = 1.000E+00
  IAS(IR,ISS),ISS=1,NAS(IR)
 1        4       13       16       25       34
  IAR(IR,ISS),ISS=1,NAS(IR)
999       4      999        2      999      999
  REGION NUMBER IR =  2     NAS =  6    IMIX =  1     IMPORT =        1     WCO =  0.600E-02    DNF = 1.000E+00
  IAS(IR,ISS),ISS=1,NAS(IR)
 2        5       16       19       26       35
  IAR(IR,ISS),ISS=1,NAS(IR)
999       5        1        3      999      999
  REGION NUMBER IR =  3     NAS =  6    IMIX =  1     IMPORT =        1     WCO =  0.600E-02    DNF = 1.000E+00
  IAS(IR,ISS),ISS=1,NAS(IR)
 3        6       19       22       27       36
  IAR(IR,ISS),ISS=1,NAS(IR)
999       6        2      999      999      999
  REGION NUMBER IR =  4     NAS =  6    IMIX =  1     IMPORT =        1     WCO =  0.600E-02    DNF = 1.000E+00
  IAS(IR,ISS),ISS=1,NAS(IR)
 4        7       14       17       28       37
  IAR(IR,ISS),ISS=1,NAS(IR)
 1        7      999        5      999      999
  REGION NUMBER IR =  5     NAS =  6    IMIX =  2     IMPORT =        1     WCO =  0.600E-02    DNF = 1.000E+00
  IAS(IR,ISS),ISS=1,NAS(IR)
 5        8       17       20       29       38
  IAR(IR,ISS),ISS=1,NAS(IR)
 2        8        4        6      999      999
  REGION NUMBER IR =  6     NAS =  6    IMIX =  1     IMPORT =        1     WCO =  0.600E-02    DNF = 1.000E+00
  IAS(IR,ISS),ISS=1,NAS(IR)
 6        9       20       23       30       39
  IAR(IR,ISS),ISS=1,NAS(IR)
 3        9        5      999      999      999
  REGION NUMBER IR =  7     NAS =  6    IMIX =  1     IMPORT =        1     WCO =  0.600E-02    DNF = 1.000E+00
  IAS(IR,ISS),ISS=1,NAS(IR)
 7       10       15       18       31       40
```

```
  IAR(IR,ISS),ISS=1,NAS(IR)
4       999       999         8       999       999
  REGION NUMBER IR =  8      NAS =  6    IMIX =  1      IMPORT =        1      WCO =  0.600E-02    DNP =  1.000E+00
  IAS(IR,ISS),ISS=1,NAS(IR)
8        11        18        21        32        41
  IAR(IR,ISS),ISS=1,NAS(IR)
5       999         7         9       999       999
  REGION NUMBER IR =  9      NAS =  6    IMIX =  1      IMPORT =        1      WCO =  0.600E-02    DNP =  1.000E+00
  IAS(IR,ISS),ISS=1,NAS(IR)
9        12        21        24        33        42
  IAR(IR,ISS),ISS=1,NAS(IR)
6       999         8       999       999       999
  SYMMETRY SURFACES
1         4         5         8

  ITALR(I),I=1,NTALR
0
REGION DEPENDENT FLUX ESTIMATOR OPTION OVERRIDE
0
ENERGY GROUP FLUX ESTIMATOR OPTION
1         1         1         1         1         1         1         1         1         1         1         1
1         1         1         1         1         1         1         1

  ITALSS(I),I=1,NTALSS
29        38
  MIX NUMBER IM =  1      NMAT(IM) =  3
  IMAT(I,IM),I=1,NMAT(IM)
10                  110                 130
  DENS(I,IM),I=1,NMAT(IM)
0.567600E-01     0.354800E-01     0.141900E-01
  MIX NUMBER IM =  2      NMAT(IM) =  1
  IMAT(I,IM),I=1,NMAT(IM)
10
  DENS(I,IM),I=1,NMAT(IM)
0.100000E-06

  TB(IT),IT=1,NT
0.100000E+09

  W(IG),IG=1,NG
0.100000E+01     0.100000E+01     0.100000E+01     0.100000E+01     0.100000E+01     0.100000E+01
0.100000E+01     0.100000E+01     0.100000E+01     0.100000E+01     0.100000E+01     0.100000E+01
0.100000E+01     0.100000E+01     0.100000E+01     0.100000E+01     0.100000E+01     0.100000E+01
0.100000E+01     0.100000E+01

  CHIP(IG),IG=1,NG
0.0              0.0              0.0              0.0              0.0              0.0
0.0              0.0              0.0              0.0              0.0              0.0
0.0              0.0              0.0              0.0              0.0              0.0
0.0              0.0

 MICROSCOPIC CROSS SECTIONS FOR MATERIAL     10  FOR ISCAT=  0
          P0  HYDROGEN CROSS-SECTIONS

 MICROSCOPIC CROSS SECTIONS FOR MATERIAL     10  FOR ISCAT=  1
```

P1 HYDROGEN CPOSS-SECTIONS

MICROSCOPIC CROSS SECTIONS FOR MATERIAL 10 FOR ISCAT= 2
P2 HYDROGEN CROSS-SECTIONS

MICROSCOPIC CROSS SECTIONS FOR MATERIAL 10 FOR ISCAT= 3
P3 HYDROGEN CROSS-SECTIONS

MICROSCOPIC CROSS SECTIONS FOR MATERIAL 110 FOR ISCAT= 0
P0 CARBON 12 CROSS-SECTIONS

MICROSCOPIC CROSS SECTIONS FOR MATERIAL 110 FOR ISCAT= 1
P1 CARBON 12 CROSS-SECTIONS

MICROSCOPIC CROSS SECTIONS FOR MATERIAL 110 FOR ISCAT= 2
P2 CARBON 12 CROSS-SECTIONS

MICROSCOPIC CROSS SECTIONS FOR MATERIAL 110 FOR ISCAT= 3
P3 CARBON 12 CROSS-SECTIONS

MICROSCOPIC CROSS SECTIONS FOR MATERIAL 130 FOR ISCAT= 0
P0 OXYGEN 16 CROSS-SECTINS

MICROSCOPIC CROSS SECTIONS FOR MATERIAL 130 FOR ISCAT= 1
P1 OXYGEN 16 CROSS-SECTINS

MICROSCOPIC CROSS SECTIONS FOR MATERIAL 130 FOR ISCAT= 2
P2 OXYGEN 16 CROSS-SECTINS

MICROSCOPIC CROSS SECTIONS FOR MATERIAL 130 FOR ISCAT= 3
P3 OXYGEN 16 CROSS-SECTINS

ANDY TEST PROGRAM 4A FINITE MODEL EDGE TEST
SETUP TIME FOR THIS PROBLEM = 0.0 SECONDS

SOURCE POSITION= -.787400E+00

	WEIGHT	X	Y	Z	UX	UY	UZ	IR	IG	IHIT	NCOL	IST	ISPL
BOUNDARY	1.0000E+00	-1.2670E-01	-3.3508E-02	3.3266E+01	-2.5472E-03	1.5157E-02	-9.9988E-01	4	4	4	0	1	0
COLLISION	8.3202E-01	-1.2904E-01	-1.9571E-02	3.2346E+01	5.7822E-02	-6.8879E-01	7.2265E-01	4	4	0	1	1	0
BOUNDARY	8.3202E-01	-1.2777E-01	-3.4685E-02	3.2362E+01	5.7822E-02	-6.8879E-01	7.2265E-01	1	4	4	1	1	0
REFLECTION	8.3202E-01	-1.2515E-01	-6.5892E-02	3.2395E+01	5.7822E-02	6.9067E-01	7.2085E-01	1	4	1	1	1	0
BOUNDARY	8.3202E-01	-1.2253E-01	-3.4600E-02	3.2427E+01	5.7822E-02	6.9067E-01	7.2085E-01	4	4	4	1	1	0
BOUNDARY	8.3202E-01	-1.1675E-01	3.4506E-02	3.2500E+01	5.7822E-02	6.9067E-01	7.2085E-01	7	4	7	1	1	0
COLLISION	2.1956E+00	-1.1774E-01	-5.4225E-02	3.4632E+01	-9.2715E-01	-3.7333E-01	-3.1841E-02	1	14	0	1	2	0
REFLECTION	2.1956E+00	-1.2596E-01	-5.7534E-02	3.4632E+01	9.2909E-01	-3.7333E-01	-3.7047E-02	1	14	13	1	2	0
REFLECTION	2.1956E+00	-1.1240E-01	-6.2980E-02	3.4632E+01	9.2909E-01	3.7574E-01	-3.9649E-02	1	14	1	1	2	0
BOUNDARY	2.1956E+00	-9.4712E-02	-5.5825E-02	3.4631E+01	9.2909E-01	3.7574E-01	-3.9649E-02	2	14	16	1	2	0
BOUNDARY	2.1956E+00	-3.5144E-02	-3.1734E-02	3.4628E+01	9.2909E-01	3.7574E-01	-3.9649E-02	5	14	5	1	2	0
BOUNDARY	2.1956E+00	9.4733E-02	2.0790E-02	3.4623E+01	9.2909E-01	3.7574E-01	-3.9649E-02	6	14	20	1	2	0
BOUNDARY	2.1956E+00	1.2182E-01	3.1743E-02	3.4621E+01	9.2909E-01	3.7574E-01	-3.9649E-02	9	14	9	1	2	0
REFLECTION	2.1956E+00	1.2599E-01	3.3430E-02	3.4621E+01	-9.3101E-01	3.7574E-01	-3.4444E-02	9	14	24	1	2	0
BOUNDARY	2.1956E+00	9.4739E-02	4.6041E-02	3.4620E+01	-9.3101E-01	3.7574E-01	-3.4444E-02	8	14	21	1	2	0
BOUNDARY	1.0000E+00	-1.1544E-01	-3.3508E-02	3.3266E+01	-2.3208E-03	1.5157E-02	-9.9988E-01	4	4	4	0	3	0
BOUNDARY	1.0000E+00	-1.2666E-01	3.9806E-02	2.8429E+01	-2.3208E-03	1.5157E-02	-9.9988E-01	7	4	7	0	3	0
COLLISION	7.6850E-02	-1.2961E-01	5.9013E-02	2.7162E+01	7.9018E-01	-6.1078E-01	5.0514E-02	7	5	0	1	3	0
BOUNDARY	7.6850E-02	-1.1416E-01	4.7075E-02	2.7163E+01	7.9018E-01	-6.1078E-01	5.0514E-02	8	5	18	1	3	0

```
BOUNDARY     7.6850E-02 -1.0689E-01  4.1454E-02  2.7163E+01  7.9018E-01 -6.1078E-01  5.0514E-02      5     5     8     1     3     0
BOUNDARY     7.6350E-02  3.6168E-04 -4.1445E-02  2.7170E+01  7.9018E-01 -6.1078E-01  5.0514E-02      2     5     5     1     3     0
REFLECTION   7.6850E-02  4.0786E-02 -7.2692E-02  2.7173E+01  7.9018E-01  6.1284E-01  4.7913E-02      2     5     2     1     3     0
BOUNDARY     7.6850E-02  8.1083E-02 -4.1439E-02  2.7175E+01  7.9018E-01  6.1284E-01  4.7913E-02      5     5     5     1     3     0
BOUNDARY     7.6850E-02  1.1412E-01 -1.5815E-02  2.7177E+01  7.9018E-01  6.1284E-01  4.7913E-02      6     5    20     1     3     0
REFLECTION   7.6850E-02  1.4537E-01  8.4179E-03  2.7179E+01 -7.9337E-01  6.1284E-01  5.3115E-02      6     5    23     1     3     0
BOUNDARY     7.6850E-02  1.1411E-01  3.2562E-02  2.7181E+01 -7.9337E-01  6.1284E-01  5.3115E-02      5     5    20     1     3     0
BOUNDARY     7.6850E-02  1.0263E-01  4.1430E-02  2.7182E+01 -7.9337E-01  6.1284E-01  5.3115E-02      8     5     8     1     3     0
BOUNDARY     1.0000E+00 -1.0981E-01 -3.3508E-02  3.3266E+01 -2.2076E-03  1.5157E-02 -9.9988E-01      4     4     4     0     4     0
BOUNDARY     1.0000E+00 -1.2048E-01  3.9806E-02  2.8429E+01 -2.2076E-03  1.5157E-02 -9.9988E-01      7     4     7     0     4     0
REFLECTION   1.0000E+00 -1.2546E-01  7.3993E-02  2.6174E+01 -2.2076E-03 -1.7760E-02 -9.9984E-01      7     4    10     0     4     0
COLLISION   -1.0598E-01 -1.2711E-01  6.0716E-02  2.5426E+01 -9.9197E-01 -1.0991E-01 -6.2632E-02      7     4     0     1     4     0
REFLECTION  -1.0598E-01 -1.4994E-01  5.8187E-02  2.5425E+01  9.9261E-01 -1.0991E-01 -6.7829E-02      7     4    15     1     4     0
BOUNDARY    -1.0598E-01 -1.1869E-01  5.4728E-02  2.5423E+01  9.9261E-01 -1.0991E-01 -6.7829E-02      8     4    18     1     4     0
BOUNDARY    -1.0598E-01 -1.9366E-02  4.3729E-02  2.5416E+01  9.9261E-01 -1.0991E-01 -6.7829E-02      5     4     8     1     4     0
BOUNDARY    -1.0598E-01  1.1873E-01  2.8438E-02  2.5407E+01  9.9261E-01 -1.0991E-01 -6.7829E-02      6     4    20     1     4     0
REFLECTION  -1.0598E-01  1.4999E-01  2.4977E-02  2.5404E+01 -9.9323E-01 -1.0991E-01 -6.2632E-02      6     4    23     1     4     0
BOUNDARY    -1.0598E-01  1.1874E-01  2.1519E-02  2.5402E+01 -9.9323E-01 -1.0991E-01 -6.2632E-02      5     4    20     1     4     0
BOUNDARY    -1.0598E-01 -1.1878E-01 -4.7657E-03  2.5387E+01 -9.9323E-01 -1.0991E-01 -6.2632E-02      4     4    17     1     4     0
REFLECTION  -1.0598E-01 -1.5004E-01 -8.2244E-03  2.5385E+01  9.9382E-01 -1.0991E-01 -6.7829E-02      4     4    14     1     4     0
BOUNDARY    -1.0598E-01 -1.1879E-01 -1.1680E-02  2.5383E+01  9.9382E-01 -1.0991E-01 -6.7829E-02      5     4    17     1     4     0
BOUNDARY    -1.0598E-01  1.1884E-01 -3.7960E-02  2.5367E+01  9.9382E-01 -1.0991E-01 -6.7829E-02      6     4    20     1     4     0
*** TRAJECTORY PROJECTION ONTO BOUNDARY OF SURFACE SEGMENT ***      INTERSECTION OF SURFACES   1 AND   7
**********                                  TERMINATION                                                          **********
                                    HISTORY RETRACED AND EXPUNGED
                                       PRINT LAST 6 EVENTS
REFLECTION  -7.6138E-01  5.1979E-02  6.4944E-02  3.3123E+01  5.5583E-01 -6.6291E-01  5.0641E-01      8     4    11     1   721     0
BOUNDARY    -7.6138E-01  7.8207E-02  3.3663E-02  3.3147E+01  5.5583E-01 -6.6291E-01  5.0641E-01      5     4     8     1   721     0
BOUNDARY    -7.6138E-01  9.8527E-02  9.4276E-03  3.3165E+01  5.5583E-01 -6.6291E-01  5.0641E-01      6     4    20     1   721     0
REFLECTION  -7.6138E-01  1.2970E-01 -2.7755E-02  3.3194E+01 -5.6015E-01 -6.6291E-01  5.1090E-01      6     4    23     1   721     0
BOUNDARY    -7.6138E-01  1.2477E-01 -3.3596E-02  3.3198E+01 -5.6015E-01 -6.6291E-01  5.1090E-01      3     4     6     1   721     0
REJECTION   -7.6138E-01  1.2477E-01 -3.3596E-02  3.3198E+01 -5.6015E-01 -6.6291E-01  5.1090E-01      3     4     0     1   721     0
X,Y VALUES ALTERED DUE TO TERMINATION OLD X,Y  NEW X,Y=   0.4076E-01   0.2174E-01   0.4130E-01   0.2174E-01
*** TRAJECTORY PROJECTION ONTO BOUNDARY OF SURFACE SEGMENT ***      INTERSECTION OF SURFACES   5 AND   4
**********                                  TERMINATION                                                          **********
                                    HISTORY RETRACED AND EXPUNGED
                                       PRINT LAST 6 EVENTS
BOUNDARY    -1.0000E+00  1.3661E-02  3.1590E-02  3.4739E+01  2.8301E-04  1.6967E-02 -9.9986E-01      8     4     8     0   762     0
COLLISION   -3.2151E-01  1.3702E-02  3.4078E-02  3.4592E+01 -9.5177E-01  1.9705E-01  2.3518E-01      8     4     0     1   762     0
BOUNDARY    -3.2151E-01 -9.4742E-02  5.6530E-02  3.4619E+01 -9.5177E-01  1.9705E-01  2.3518E-01      7     4    18     1   762     0
REJECTION   -3.2151E-01 -9.4742E-02  5.6530E-02  3.4619E+01 -9.5177E-01  1.9705E-01  2.3518E-01      7     4     0     1   762     0
X,Y VALUES ALTERED DUE TO TERMINATION OLD X,Y  NEW X,Y=   0.1359E-01   0.2717E-01   0.1304E-01   0.2717E-01
*** PARTICLE PRESUMED LOST IE. NO POSITIVE INTERSECTIONS OF TRAJ. WITH BOUNDING SEGMENTS S.T. DTOL.LT.DTRY.LT.DIMAX ***
**********                                  TERMINATION                                                          **********
                                    HISTORY RETRACED AND EXPUNGED
                                       PRINT LAST 6 EVENTS
REFLECTION  -1.0000E+00 -1.3826E-02  6.3599E-02  3.4156E+01 -2.8301E-04 -2.0024E-02 -9.9980E-01      8     4    11     0   941     0
COLLISION   -5.0592E+00 -1.4240E-02  3.4257E-02  3.2691E+01  2.2512E-01 -2.7763E-01 -9.3394E-01      8     4     0     1   941     0
REJECTION   -5.0592E+00 -1.4240E-02  3.4257E-02  3.2691E+01  2.2512E-01 -2.7763E-01 -9.3394E-01      8     4     0     1   941     0
X,Y VALUES ALTERED DUE TO TERMINATION OLD X,Y  NEW X,Y=  -0.1359E-01   0.4891E-01  -0.1304E-01   0.4891E-01
    3 HISTORIES REJECTED
   ANDY TEST PROGRAM 4A FINITE MODEL EDGE TEST
IUK= 0      IGCUT= 14      ICT= 0      XNP=  0.1058E+04          TPROB=     0.0  SECONDS
          RESULTS FOR CASE WITH NKRN= 3413
```

```
          RESULTS FOR TIME INTERVAL     1       TIME = 1.0000E+08

          WISP FOR SEGMENT  29      TOTAL WEIGHT =    0.0              DEV.=  0.0                    HISTORIES      TOTAL =      0
    0.0             0.0             0.0             0.0             0.0             0.0          0        0        0        0        0
    0.0             0.0             0.0             0.0             0.0             0.0          0        0        0        0        0
    0.0             0.0                                                                          0        0
          WISN FOR SEGMENT  29      TOTAL WEIGHT =    0.0              DEV.=  0.0                    HISTORIES      TOTAL =      0
    0.0             0.0             0.0             0.0             0.0             0.0          0        0        0        0        0
    0.0             0.0             0.0             0.0             0.0             0.0          0        0        0        0        0
    0.0             0.0                                                                          0        0

          WISP FOR SEGMENT  38      TOTAL WEIGHT =    2.219E+00        DEV.=  0.6270E+00         HISTORIES      TOTAL =      9
    0.0             0.0             0.0             2.312E+00       2.448E-01      -6.656E-01    0        0        5        1        1
 -1.223E-01         0.0             4.501E-01       0.0             0.0             0.0          1        0        1        0        0
    0.0             0.0                                                                          0        0
          WISN FOR SEGMENT  38      TOTAL WEIGHT =    0.0              DEV.=  0.0                    HISTORIES      TOTAL =      0
    0.0             0.0             0.0             0.0             0.0             0.0          0        0        0        0        0
    0.0             0.0             0.0             0.0             0.0             0.0          0        0        0        0        0
    0.0             0.0                                                                          0        0
     IST      ISPLC      ISPLO      NHS       NCOL       NDEL    NESCEL    NENCUT    NESCAP    NKIMP    NKRROU    NKTIME
     1058          0          0     1058        853          0      1020        13        21        0         4         0
HISTORY GAINS - LOSSES =      0

        WESCEL          WENCUT          WESCAP          WKIMP           WKRROU          WCREAT
    0.994554D+03    0.400005D+02    0.129842D+02    0.0             -0.389803D-03   -0.104617D+02

        WKTIME
    0.0
WEIGHT GAINS - LOSSES =    0.20893D-03


          FINAL VALUE OF KRN
      911653503
ICELX(I) I=1,NXC
       36      45      59      99     208      16     196      79      49      34
       27      20
ICELY(I) I=1,NYC
        1       1       2       3       3       3       3       3       3       3
        3       3       4       6       5       5       6       7       7       9
        9      10       9      14      16      22      27      38    1051     963
```

APPENDIX C. SPECIFYING ANDY GEOMETRY

Consider the cylinder below with a radius of r=1 and a length 1 and centered on the z-axis.

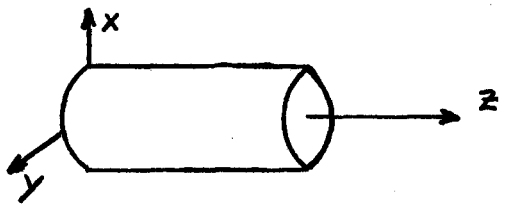

Figure C.1. Sample Geometry

In order to specify the cylinder we need three surfaces, the two end caps, and the can wall. In ANDY, one uses standard equations for surfaces and specify a particular surface by a surface type number and the correspondigng parameters. For example, let surface 1 be the cylinder. Since it is a cylinder parallel to the Z-axis,parameters for the x and y position and the radius are required. So surface 1 is specified:

Surface	Type	C.L. X position	C.L. Y position
1	Z-Cylinder	0.0	0.0

Radius
1.0

In the actual code input the type is specified by a number. These are given in Owen Deutsch's User's guide to "ANDY" [3], and in Appendix D on COLLUM.ANDY input specifications.

The end caps lie on x,y planes and are given by:

Surface	Type	Z Coordinate
2	x-y plane	0.0
3	x-y plane	1.0

Next the surface segments must be specified. In this case there are three, one for each surface. Generally, there are many more segments then surfaces. Consider the cylinder again. The surface segment is defined by the surface it resides on and the senses of the bounded surfaces. The sense is the point which indicates which side of the boundary surface the bounded surface is on. In this case:

Surface Segment	On Surface	Boundary Surface and Sense
1	1	+2, -3
2	2	-1
3	3	-1

The senses are positive if they are in the direction of the typical normals of a surface. For example, if for surface segment 2, +1 had beengiven instead of -1 the surface would have been the infinite plane without the inside of the cylinder.

Finally, one is ready to specify the regions. Regions are specified by the region number, the surface segments bounding it, and the regions on the opposite side of each bounding segment. When the segment forms the boundary of problem geometry specifications, 999 is given for the region specification opposite the

surface segment. Thus, region 1 in this problem is given by:

Region	Surface Segments		
1	1	2	3
	Corresponding Region Opposite		
	999	999	999

Each region also has associated with it a code for the type of material.

APPENDIX D. COLLUM.ANDY INPUT DESCRIPTION

ANDY DATA INPUT DESCRIPTION

1. TITLE, TIML

18A4, F8.0

TITLE = 72 column identification for problem

TIML = execution time limit for calculation in seconds (CP time). Note: Job time limit should exceed TIML.

2. NG, NP, NING, NSCAT, NMIX, NLIBSM, NTPDEL, MCR, MTP

Note: Unless specified specified otherwise, integer formats are 12I6, real formats are 6E12.0

NG = # energy groups

NP = cross section table length

NING = position of self-scatter cross section

NSCAT = order # of anisotropic scattering tables

NMIX = # material mixtures

NLIBSM = # summing cross section tables (relates to card 18)

NTPDEL = # types of delayed particles

MCR = # materials from cards

MTP = # materials from library file

3. NREG, NSUR, NSEG, NSEGRA, NSENMA

NREG = # regions

NSUR = # surfaces

NSEG = # surface segments

NSEGRA = maximum number of surface segments per region

NSENMA = maximum number of sense relations per segment

4. NT, ITB1, NTALR, NTALSS, NIT, NMATMA, NSUM

NT = # time bins

ITB1 = # time bins of width DELT1

NTALR = # region tallies

NTALSS = # surface tallies

NIT = 0

NMATMA = maximum number of materials per mixture

NSUM = # summing tallies

5a) IUK, IGCUT, NG1, ICT, NSYMS, XNF
516, E12.5

IUK = 0 for iostropic simulation pattern
= 1 for simulation pattern represented in c.x.

(Note: for NSCAT=0, must set IUK=0)

IGCUT = energy group cutoff, i.e. particles in energy groups > IGCUT are terminated.

NG1 = # groups for cross section print

ICT = 0 to adjust particle weight by 'c' after collisions
= 1 to generate IFIX(c) histories after collisions.

XNF = normalization factor (total source weight)

NSYMS = # summetry surfaces (planar)

5b) Source Input Parameters I:Source Distribution Grid
NXB, NYB, BD XSET, YSET 2I6, E12.6

NXB = # of boxes in x direction for Fixed SOURCE subroutine initial particle distribution grid NXB*BD=X cell dimension

NYB = # boxes in y direction

BD = grid box dimension

(Note: NXB*BD and NYB*BD must equal the cell dimensions for both the random and Fixed Source subroutines

5c) Source Input II - Scan Parameters
NXC, NYC, NCEX, NCEY, XSET, YSET, YSP, YSINC, 4I6, 4E12.6

NXC = # of collimator cells in the x direction

NYC = # of collimator cells in the y direction

NCEX = initial x cell

Note add to 9.

NCPRT = 0 ship collision parameter print out.

5a (cont'd)

NCEY = initial y cell

X-SET = X inner-wall boundary value

Y-SET = Y inner-wall boundary value

YSP = initial source position minus increment
YSP + YSINC = first scan position.

YSINC = source position increment; incremental in y direction.

6. IDMAT(I), I=1, MCR (MCR > 0)

ID numbers for cross sections read from cards

7. LIBRX

18A4

72 Column identification of cross sections to be read from cards.

8. CROSS SECTIONS

FIDO Format (only repeat specification allowed)

Terminate with 'T' in column 3 following cross sections

9. NS, NKRN, MORE, NPUNCH, MCOL, NDEV, NCRX, ISTPRT, NCPRRT

NS = # histories to be started

NKRN = odd integer used to start sequence of pseudo-random numbers NKRN$\leq$999

MORE = # successive runs with NS starters, NKRN incremented by 2 to cycle through odd integers

NPUNCH = 0 skip collision parameter printout

MCOL = # collisions per history before Russian roulette

NDEV = 0→skip group deviation printout

NCRX = 0→skip micro & macro X-sect. printout

ISTPRT = history number of complete trajectory trace if non-zero.

Note: It is suggested that on initial runs more=0, npunch=0, MCOL=500, NDEV=1, NCRX=1, ISTPRT=1, NSPPRT=1.

10a. DELT1, DELT2, OFFSET, TSPLT, WDELF 74

OFFSET = width of first time bin (units of 10^{-8} seconds)

DELT1 = width of time bins 2,ITB1

DELT2 = width of time bins ITB1+1,NT

Note: DELT1, DELT2 should be set $\neq$ 0 even if NT=1

TSPLT = 0.

WDELF = tolerance level for generation of delayed particle history, i.e., generate delayed history when cumulative weight of delayed particles generated at collisions exceeds WDELF.

10b. DIMAX WCOI WSPLT

DIMAX = maximon pathlength in problem

WCOI = Russian Roulette cutoff weight, WCO=WCOI/IMPORT

WSPLT = maximum weight per history.

GEOMETRY

SURFACE DEFINITIONS

ITP	TYPE	EQUATION
1	x plane	$X - AS = 0$
2	y plane	$Y - AS = 0$
3	z plane	$Z - AS = 0$
4	sphere	$(X-AS)^2 + (Y-BS)^2+(Z-CS)^2-DS^2 = 0$
5	x cylinder	$(Y-AS)^2+(Z-BS)^2-CS^2 = 0$
6	y cylinder	$(X-AS)^2+(Z-BS)^2-CS^2 = 0$
7	z cylinder	$(X-AS)^2+(Y-BS)^2-CS^2 = 0$
8	z elliptic cylinder	$(X/AS)^2 + (Y/BS)^2 = 1$
9	skew plane	$X*BS + Y*CS + Z*DS = AS$
10	general quadratic I	$BS*X^2 + CS*Y^2 + DS*Z^2 + ES*Y + FS*Y + GS*Z - AS^2 = 0$
11	general quadratic II	$BS*(X-ES)^2 + CS*(Y-FS)^2 + DS*(Z-GS)^2 - AS^2 = 0$

Note 1: The general quadratics can be used to specify cones, parabolic, hyperbolic, elliptic surfaces, i.e., any conic section, or surface of revolution of a conic section.

Note 2: The most general quadratic includes mixed cross terms and is not presently encoded in the ANDY geometry because it is almost never used.

11. NSFC(IS), ITP(IS), AS(IS), BS(IS), CS(IS), DS(IS)
    216, 5E12.4

    ES(IS), FS(IS), GS(IS) only if ITP>8
    6E12.4

NSFC = surface number
ITP = surface type
AS,BS, CS, DS, ES, FS, GS = surface parameters as described in surface definitions

Repeat this one or two card sequence for all surfaces, i.e., IS = 1, NSUR

12. INS(ISS), IDS(ISS), NSEN(ISS)
    (IDEN(ISS, IS1), IS1=1, NSEN) only if NSEN(ISS)>0

INS = surface segment number
IDS = # of surface on which ISSth segment resides
NSEN = # of sense relations of ISSth segment
IDEN = signed surface numbers which describe extent of ISSth segment by indicating sense with respect to intersecting surfaces.

Repeat this sequence for all segments
i.e., ISS = 1, NSEG

13. NAS(IR), IMIX(IR), IMPORT(IR), DNF(IR)
    216, I12, 2E12.6
    IAS(IR,ISS), ISS=1,NAS(IR)
    IAR(IR,ISS), ISS=1,NAS(IR)

Note: to define a region outside use a # greater than NREG (check if equal to STM70 in PREP) (Now at 999).

NAS = # surface segments bounding region IR

IMIX = material (mixture) number for region IR

IMPORT = 'importance' of region IR used to determine particle splitting and Russian Roulette, and to kill particles by IMPORT = 0

DNF = density factor. Notes: In Russian Roulette and splitting use DNF L.T. 1.0E-09 for short circuiting splitting in external vacuum regions. Normally set equal to 1.0. This density factor can also be used to model the density of a region without changing IMIX(IR) i.e., one can minimize the # of mixtures. If just the density has changed from one region to another.

DNF = 1.0E-09 simulates a vacuum region saves time by ignoring collisions

IAS = surface segment numbers for segments which bound region IR

IAR = region numbers for regions on other side of segment IAS from region IR.

Repeat this three card sequence for all region, IR=1, NREG

14. IDEC (NSYMS) Symmetry Specifications
presently skew plane reflection is limited to X,Z Y-Z and X,Y reflection see coding in BUSY for more detail.

Note: Enter blank card if NTALR=0.

15a. ITALR(I), I=1,NTALR

region numbers of region tallies

Note: Enter blank card if NTALR=0.

15b. JTALR ITALR(I=1), ITALR (I=NTALR)

JTALR = +1 to force collision tally in region (I) for all groups

JTALR = -1 to force path length tally

15c. IGTALR(I6 = 1), IGTAL-R(IG=NG)

IGTALR = +1 collision tally by group

IGTALR = -1 path length tally by group

16. ITALSS(I), I=1, NTALSS

surface segment numbers for surface tallies

Note: Enter blank card if NTALSS=0.

17. NMAT(IM)

IMAT(I,IM), I=1, NMAT

DENS(I,IM), I=1, NMAT

NMAT = # of elements for mixture IM

IMAT = ID # for I^{th} element in mixture iM

DENS = number density (nucleii/cm^3 x 10^{-24}) for I^{th} element in mixture IM.

Repeat this sequence for all mixture, IM=1,NMIX

Note: The ANDY cross section mixing scheme differs from the ANISN 'mix table' in that only one specification is required to mix an element into a mixture. The ANISN mix scheme requires the user to separately mix each 'table' of a multitable PN set for each element in a mixture, i.e. the cross section ID # is associated with an element, rather than with a particular table of an element as far as the user is concerned.

18. DENSM(I,ISUM), I=1,NLIBSM only if NSUM>0
IRORS(ISUM), ISUMTY(ISUM) only if NSUM>0

DENSM = 'density' of I^{th} summing cross section in integral sum number ISUM
IRORS = 0 to indicate region sum
= 1 to indicate surface sum
ISUMTY = region or surface segment #1 for $ISUM^{th}$ sum

19. V(IG), IG=1,NG
V = velocity of group IG (units of 10^8 cm/sec)

20. CHIP(IG), IG=1,NG
CHIP = cumulative distribution fission spectrum
i.e. CHIP(NG) = 1.

21. ((CHID(ITPDEL,IG),IG=1,NG),ITPDEL=1,NTPDEL) only if NTPDEL>0
((DELPC ITPDEL,IG),IG=1,NG),ITPDEL=1,NTPDEL) Only if NTPDEL >0
(TD(ITPDEL),ITPDEL=1,NTPDEL)
CHID = delayed particle spectra (cumulative distribution) for each of the NTPDEL types of delayed particles
DELPC = delayed particle fraction of yield/collision into each energy group for each of the NTPDEL types of delayed part.
TD = mean delay time (time constants) for each of the NTPDEL types of delayed particles 9units of 10^{-8} seconds).

22. LIBRX(I), I=1,18
18A4
CL(1,IG), IG=1,NG
LIBRX = 72 column identifier for I^{th} summing cross section
CL = I^{th} set of summing cross sections
Repeat this sequence for all (NLIBSM) sets of summing cross sections.

APPENDIX E. COLLUM. ANDY LISTING

NOTE:

APPENDIX E. COLLUM. ANDY LISTING

THIS IS A COMPUTER CODE LISTING AVAILABLE FROM THE LIBRARY UPON REQUEST. IT IS MAINTAINED UNDER PFC/IR-82-1. REQUESTS CAN BE MADE FROM:

Beverly Colby
Library
Plasma Fusion Center
167 Albany Street
Cambridge, MA 02139

MIT PLASMA FUSION CENTER PHYSICS DISTRIBUTION LIST

AMPC Inc., Guest, Dr. G.
Association Euratom - CEA, Dept. de Physique de Plasma et de la Fusion Controle, France
Association Euratom - CEA, France, Brifford, Dr. G.
Austin Research Associates
Australian National University, Australia, Hamberger, S.M.
Bank of Tokyo, Ltd., Japan, Azuma, Mr. Katsuhiko
Central Research Institute for Physics, Hungary, Kostka, P.
CNEN - Centro di Frascati, Italy
CNR - Centro di Studio sui Gas Ionizzati, Italy, Ortolani, S.
College of William and Mary, Montgomery, Prof. David
Columbia University, Schlesinger, Prof. Perry
Consoli, T., France
Cornell University, Fleischmann, Prof. H.
Cornell University, Laboratory for Plasma Studies
Dewar, R.L., New Jersey
Division of Research and Laboratories, Austria, Frolov, V.
Ecole Royale Militaire, Belgium, Vandenplas, P.E.
EG&G Idaho, Inc., Crocker, Mr. J.
FOM-Institute for Plasma Physics, Netherlands
General Atomic Company, Fusion Energy Division
Hiroshima University, Japan, Nishikawa, Prof. K.
INESCO, Inc., Wagner, Dr. C.
Inst. of Physics, Warsaw University Branch, Poland, Brzosko, J.S.
Inst. Nacional de Invest. Nucleares, Mexico, Salas, J.S. Ramos
Japan Atomic Energy Research Institute, Japan, Mori, Dr. S.
JET Joint Undertaking, United Kingdom
KFA Julich, Institut fur Plasmaphysik, FRG
Kharkov Physical-Technical Institute, USSR, Tolok, Dr. V.T.
Kurchatov Institute, USSR, Eliseev, Dr. G.A.
Kurchatov Institute of Atomic Energy, USSR
Kyoto University, Japan, Uo, Prof. K.
Kyushu University, Japan, Itoh, Prof. Satoshi
Lawrence Berkeley Laboratory
Lawrence Livermore Laboratory, Magnetic Fusion Energy Div.
Lebedev Institute of Physics, USSR, Rabinovich, Dr. M.S.
Lockheed Palo Alto Research Laboratory, Siambis, John
Los Alamos Scientific Laboratory, CTR Division
Max-Planck-Institut fur Plasmaphysik, FRG
Nagoya University,Institute of Plasma Physics, Japan
National University of Singapore, Singapore, Jones, Dr. R.
Naval Research Laboratory, Plasma Physics Division
Naval Surface Weapons Center, Uhm, Prof. Han S.
New York University, Courant Inst. of Mathematical Sci.
Nuclear Research Institute, Czechoslovakia, Bartosek, V.
Nuclear Service Corporation, Naymark, Mr. Sherman
Oak Ridge National Laboratory, Fusion Energy Division
Osaka University, Japan, Ito, Prof. H.
Palumbo, D., Belgium
Physics International Group, Benford, Dr. Jim
Princeton University, Plasma Physics Laboratory
Rijksuniversiteit Gent, Belgium, Verheest, F.
Riso National Laboratory, Denmark, Jensen, V.O.
Royal Institute of Technology, Sweden, Lehnert, B.P.
Ruhr-Universitat, FRG, Kunze, H.-J.
S. Kaliski Inst. of Plasma Phys. and Laser Microfusion, Poland, Fiedorowicz, H.
Sandia Research Laboratories, Plasma Physics Division
Science Applications, Inc., CA
Science Applications, Inc., MD, Dean, Dr. Stephen
Science Applications, Inc., VA, Drobot, Dr. Adam
Science Council of Japan, Japan, Fushimi, K.
Scientific Res. Inst. of Electro-Physical Apparatus, USSR, Glukhikh, Dr. V.A.
Siberian Section of the USSR Academy of Sciences, USSR
Soreq Nuclear Research Center, Israel, Rosenblum, M.
Stanford University, Buneman, Prof. O.
Technion, Israel, Rosenau, P.
Tel-Aviv University, Israel, Cuperman, S.
Tohoku University, Japan, Nagao, Prof. S.
TRW, Defense and Space Systems
UKAEA, Culham Laboratory, England
U.S. Dept. of Energy, Office of Fusion Energy
U.S. Dept. of Energy, Trivelpiece, Dr. A.W.
Universitat Innsbruck, Austria, Cap, F.
Universitat Stuttgart, FRG, Wilhelm, R.
Universite de Montreal, Canada, Paquette, G.
Universite Libre de Bruxelles, Belgium, Balescu, R.C.
University of Alberta, Canada, Offenberger, A.A.
University of Bergen, Norway, Berge, G.
University of B.C., Canada, Curzon, Dr. F.
University of California at Berkeley:
    Dept. of Electrical Eng. and Computer Sci.
    Dept. of Physics
University of California at Irvine, Department of Physics
University of California at L.A.:
    Dept. of Electrical Eng.
    Dept. of Physics
University of California at L.A., Conn, Dr. Robert W.
University of California at L.A., Kastenberg, William E.
University of California at L.A., Taylor, Dr. Robert
University of California at San Diego, Dept. of Physics
University of Illinois, Choi, Prof. Chan
University of Malay, Malaysia, Lee, S.
University of Maryland:
    Dept. of Electrical Eng.
    Dept. of Physics
    Inst. for Physical Sciences and Technology
University of Michigan, Getty, Prof. Ward D.
University of Nairobi, Kenya, Malo, J.O.
University of Natal, South Africa, Hellberg, M.A.
University of Rochester, Simon, Prof. Albert
University of Saskatchewan, Canada, Hirose, A.
University of Texas at Austin:
    Center for Energy Studies
    Dept. of Physics
University of Texas at Austin Kochanski, Dr. Ted
University of Tokyo, Japan, Uchida, Prof. T.
University of Tsukuba, Japan, Inutake, Dr. M.
University of Waikato, New Zealand, Hosking, R.J.

University of Wisconsin, Callen, Dr. Jim
University of Wisconsin, Tataronis, Dr. J.
Yale University, Dept. of Applied Science

PFC BASE MAILING LIST

Argonne National Laboratory, TIS, Reports Section
Associazione EURATOM - CNEN Fusione, Italy, The Librarian
Battelle-Pacific Northwest Laboratory, Technical Info Center
Brookhaven National Laboratory, Research Library
Central Research Institute for Physics, Hungary, Preprint Library
Chinese Academy of Sciences, China, The Library
The Flinders University of S.A., Australia, Jones, Prof. I.R.
General Atomic Co., Library
General Atomic Co., Overskei, Dr. D.
International Atomic Energy Agency, Austria,
Israel Atomic Energy Commission, Soreq Nucl. Res. Ctr., Israel
Kernforschungsanlage Julich, FRG, Zentralbibliothek
Kyushu University, Japan, Library
Lawrence Berkeley Laboratory, Library
Lawrence Livermore Laborary, Technical Info Center
Max-Planck-Institut fur Plasma Physik, FRG, Main Library
Nagoya University, Institute of Plasma Physics, Japan
Oak Ridge National Laboratory, Fusion Energy Div. Library
Oak Ridge National Laboratory, Derby, Roger
Physical Research Laboratory, India, Sen, Dr. Abhijit
Princeton University, PPL Library
Rensselaer Polytechnic Institute, Plasma Dynamics Lab.
South African Atomic Energy Board, S. Africa, Hayzen, Dr. A.
UKAEA, Culham Laboratory, England, Librarian
US Department of Energy, DOE Library
Universite de Montreal, Lab. de Physique des Plasmas, Canada
University of Innsbruck, Inst. of Theoretical Physics, Austria
University of Saskatchewan, Plasma Physics Lab., Canada
University of Sydney, Wills Plasma Physics Dept., Australia
University of Texas at Austin, Fusion Res. Ctr., Library
University of Wisconsin, Nucl. Eng. Dept., UW Fusion Library

INTERNAL MAILINGS

MIT Libraries
Industrial Liaison Office
G. Bekefi, A. Bers, D. Cohn, B. Coppi, R.C. Davidson,
T. Dupree, S. Foner, J. Freidberg, M.O. Hoenig, M. Kazimi,
L. Lidsky, E. Marmar, J. McCune, J. Meyer, D.B. Montgomery,
J. Moses, D. Pappas, R.R. Parker, N.T. Pierce, P. Politzer,
M. Porkolab, R. Post, H. Praddaude, D. Rose, J.C. Rose,
R.M. Rose, B.B. Schwartz, L.D. Smullin, R. Temkin, P. Wolff,
T-F. Yang